Hamilton Andrew, K (Orcid ID: 0000-0002-2286-1472)
Laval Bernard (Orcid ID: 0000-0002-4810-9246)
Albers Sam, J (Orcid ID: 0000-0002-9270-7884)
Allchin Michael, Ian (Orcid ID: 0000-0002-6108-5189)
Carmack Eddy, Clark (Orcid ID: 0000-0001-6870-7772)
Dery Stephen, Jacques (Orcid ID: 0000-0002-3553-8949)
French Todd, D. (Orcid ID: 0000-0002-4834-7463)
Granger Brody, K (Orcid ID: 0000-0001-7475-5762)
Owens Philip, N (Orcid ID: 0000-0001-8924-7437)
Vagle Svein (Orcid ID: 0000-0002-0098-2329)

Seasonal turbidity linked to physical dynamics in a deep lake following the catastrophic 2014 Mount Polley mine tailings spill

Andrew K. Hamilton[1†], Bernard E. Laval[1], Ellen L. Petticrew[2,3], Sam J. Albers[2], Michael Allchin[3], Susan A. Baldwin[4], Eddy C. Carmack[5], Stephen J. Déry[6], Todd D. French[2,3,6], Brody Granger[1], Kelly E. Graves[1], Philip N. Owens[3,6], Daniel T. Selbie[7], and Svein Vagle[5]

[1]Department of Civil Engineering, University of British Columbia, Vancouver, BC, Canada

[2]Geography Program, University of Northern British Columbia, Prince George, BC, Canada

[3]Quesnel River Research Centre, University of Northern British Columbia, Likely, BC, Canada

[4]Chemical and Biological Engineering, University of British Columbia, Vancouver, BC, Canada

[5]Institute of Ocean Sciences, Fisheries and Oceans Canada, Sidney, BC, Canada

[6]Environmental Science Program, University of Northern British Columbia, Prince George, BC, Canada

This article has been accepted for publication and undergone full peer review but has not been through the copyediting, typesetting, pagination and proofreading process which may lead to differences between this version and the Version of Record. Please cite this article as doi: 10.1029/2019WR025790

[7]Fisheries and Oceans Canada, Pacific Region, Science Branch, Cultus Lake Salmon Research Laboratory, Cultus Lake, BC, Canada

Corresponding author: Andrew Hamilton (akhamilt@ualberta.ca)

†Current address: Earth and Atmospheric Sciences, University of Alberta, Edmonton, AB, Canada

Key Points

- Quesnel Lake turned bright green when turbid spill material trapped in the hypolimnion mixed to the surface during autumn 2014 turnover
- Seasonal turbidity increases every year since the spill are likely due to mobilization of spill-related bottom sediment by internal seiches
- Physical dynamics are key to understanding the long-term impact of acute and chronic mine spills even in deep aquatic systems

Abstract

The catastrophic August 2014 Mount Polley tailings spill, the second largest ever documented, sent ~18 Mm^3 of waste plunging to the bottom of the >100 m deep West Basin of Quesnel Lake, British Columbia, a critical West Coast salmon habitat. To understand the impact of the spill on the lake, including the fate of suspended solids, we examine changes in physical water properties over 11 years (2006 – 2017) using water column profiles, moored timeseries, and satellite imagery. Contaminated waters were initially largely confined to the hypolimnion, however, during autumn 2014 turnover turbid waters were mixed to the surface, resulting in the clear-blue lake turning bright green. Twelve months after the spill the lake's temperature, conductivity, and turbidity temporarily returned to pre-spill conditions, however, initiation of mine effluent discharge in late 2015 was associated with a subsequent 15 $\mu S\ cm^{-1}$ conductivity increase above historic values. Importantly, a post-spill 1-2.5 formazin turbidity unit hypolimnetic turbidity increase was observed during spring and fall turnovers of 2015-2017, which appeared to be due to mobilization of a thin layer of unconsolidated spill-related material from the lake bed driven by large internal seiche motions. This process implies spill contaminants may be seasonally mobilized into the water column, with potentially detrimental impacts on aquatic ecology. Our findings underscore that basin-scale physical processes, including seasonal turnover and internal seiches, must be accounted for, even in deep lakes, to understand the long-term impact of the ever increasing number of tailings spills into aquatic ecosystems.

Plain Language Summary

The catastrophic failure of the Mount Polley copper and gold mine tailings pond dam in August 2014 was, at the time, the largest mine-related spill ever documented. The turbid torrent of mine waste plunged to the bottom of the pristine waters of Quesnel Lake, British Columbia, critical habitat for West Coast salmon stocks. Despite the scale of the spill, there was surprisingly little visible evidence of it at the surface of the lake in the months following. But what happened below the surface? Using eleven years of water column measurements, we show that as the lake mixed from top to bottom (called turnover) that autumn the contaminated deep water was brought to the surface, abruptly changing the color of the clear-blue lake to an abnormal bright green color – a change readily visible from space. Each year since the spill the turbidity of the lake has increased in spring and autumn during turnover,

apparently due to re-suspension of spill material off the lake bottom driven by basin-scale wave oscillations. This process, and the ongoing discharge of excess mine waste water directly into the lake, raises concerns over the seasonal mobilization of mine contaminants and their impact on aquatic ecosystems.

1. Introduction

The mining industry produces billions of tonnes of tailings waste each year that are often contained in above-ground reservoirs, or tailings dams, which are among the largest engineered structures on Earth (Azam & Li, 2010; Kossoff et al., 2014; Owen et al., 2020; Pullum et al., 2018). The earth-filled embankments of tailings dams have a global failure rate two to ten-fold that of conventional concrete and steel dams (Davies, 2001, 2002; WISE, 2020; Vogel, 2013), and the sudden release of massive volumes of waste slurry as a gravity current can have catastrophic consequences for downstream populations, infrastructure, and environments (e.g., Davies, 2001; Kraft et al., 2006; Leppänen et al., 2017; Macklin et al., 2003; Sammarco, 2004; Santamarina et al., 2019; Segura et al., 2016; Shandro et al., 2017; Van Niekerk & Viljoen, 2005). Natural water courses are the preferential runout corridors for tailings spills, and Owen et al.'s (2020) global survey of 328 active tailings dams showed that of the 55 that were rated "high-risk" for failure, all of them were located within 5 km of a waterway, underscoring the urgent need to understand the potential impacts of acute tailings spills on downstream aquatic systems.

Tailings spills involve the release of up to tens of millions of m^3 of mine process water and fine-ground sediments, often carrying high concentrations of dissolved ions, heavy metals, and various chemical compounds (Kossoff et al., 2014). When the waste plume enters an aquatic system the transport and fate of sediment and contaminants is determined by various fluid mechanic processes, including flow speeds, settling rates, and mixing dynamics. Where spills occur into river systems the suspended sediment and contaminant load can be transported large distances downstream with widespread consequences (Kossoff et al., 2014; Lásló, 2006; Macklin et al., 2003; Robertson et al., 2019; Rotta et al., 2020; Soldán et al., 2000). The majority of tailings spill impact studies have been undertaken in large river systems with relatively high flushing rates and, to a much lesser extent, in marine estuaries,

generally focusing on biological, chemical, economic, and human impacts (Babić-Mladenović et al., 2002; Fonseca do Carmo et al., 2017; Ishihara et al., 2015; Lucas, 2001; Macklin et al., 2003; Magris et al., 2019; Ruyters et al., 2011; Segura et al., 2016; Soldán et al., 2001; Veinott et al., 2003). Few studies have investigated physical processes involved in the transport and fate of dissolved and suspended contaminants, and fewer still have examined direct impacts of acute spills on longer residence-time lakes and reservoirs where much of the tailings are eventually deposited.

Understanding the dispersal and fate of tailings material, particularly fine sediments and their associated contaminants, in lakes and reservoirs is often complicated by a lack of baseline observations, the cumulative effects of long-term chronic pollution, or high natural suspended sediment loads. For example, studies examining the retention of solids, metals, and nutrients have been undertaken on the run-of-the-river Iron Gate Reservoir on the Danube River, eastern Europe, that was impacted by the Baia Mare, Romania, cyanide spill in 2000, but the reservoir has also received decades of waste water and contaminants from a population of ~80 million inhabitants of the heavily industrialized Danube watershed (Babić-Mladenović et al., 2002; Teodoru & Wehrli, 2005; Vuvovik et al., 2014). Studies on the biological and geomorphological impacts of solids and metal loadings on Lake Coeur d'Alene, Idaho, USA, which has been affected by the deposition of an estimated 75 M tons of contaminated sediments from the Bunker Hills mine, are comprehensive, however the wastes have accumulated over a century of mining (Bookstrom et al., 2001). Spills into lakes can have substantial consequences for lake physics and biota, for example, a combination of a series of acute spills and long-term leaching of saline water from the Terrafame Talvivaara mine, Finland, turned nearby Lake Kivijärvi meromictic, sediment became heavily contaminated, and phytoplankton and zooplankton communities have been significantly altered (Leppänen et al., 2017). Here, we examine the physical limnological effects of a massive tailings spill which was discharged over a short period (~1 day) into, and largely contained by, a deep lake previously undisturbed by development. Thus, not only is identification of the acute and immediate effects of the tailings dispersal relatively straightforward, but tracking the long-term dispersal and impact of spill material is possible.

On 4 August 2014, the failure of the Mount Polley Mining Corporation (MPMC) copper and gold mine tailings dam in central British Columbia (BC), Canada (Figure 1), released a ~25 Mm^3 debris flow (MPMC, 2015), at the time the largest mine tailings spill by volume ever documented (Byrne et al., 2018; WISE, 2020). The spill consisted of approximately 7.3 Mm^3 of non-acid generating tailings solids, 10.6 Mm^3 of supernatant water, 6.5 Mm^3 of interstitial water, and 0.6 Mm^3 of construction materials (Byrne et al., 2018; Hudson-Edwards et al., 2019; SNC-Lavalin, 2014). The Mount Polley tailings dam (2.4 km^2) was located upstream of Quesnel Lake, a large, deep, oligotrophic fjord-lake, and the debris flow surged 9.2 km along the Hazeltine Creek channel before discharging into the lake's West Basin (WB), a semi-isolated 113 m deep sub-basin connected to the Main Basin of the lake over a 35 m deep sill near Cariboo Island (Figure 1). Ultimately, a total of 18.6 ±1.4 Mm^3 of waste solids and liquids, and scoured overburden from the creek channel plunged through the WB's thermally stratified surface waters and spread out as a subsurface plume, transforming hypolimnetic temperature from 5 °C to 7 °C, electrical conductivity from 110 to 160 μS cm^{-1}, and turbidity from <1 to >1000 formazin turbidity units (FTU; MPMC, 2016a; Petticrew et al., 2015). The spill generated a layer of waste up to 10 m thick that extended over ~1.2 km^2 in the deepest portion of the WB (below 100 m depth; MPMC 2016a), and a surficial layer of waste over an area of at least 12 km^2 (Golder Associates, 2017). Water column profiles collected in the 3-months following the spill indicated that some of the fine suspended sediments were exported westward out the Quesnel River and some transported eastward over the sill into the Main Basin by natural seiche activity (Petticrew et al., 2015), yet an estimated 30×10^6 kg of fine particles (median particle diameter of 1 μm) remained in suspension below 30 m depth in the WB as of 2 October 2014 (Petticrew et al., 2015).

Despite the magnitude of the spill and its transformative impact on the physical properties of the hypolimnion, there was surprisingly little visible evidence of it in the surface waters of Quesnel Lake owing to the strong summer thermal stratification; epilimnetic turbidity and conductivity remained comparatively low (<5 FTU and <110 μS cm^{-1}, respectively) from 20 August to 4 October 2014 (Petticrew et al., 2015). However, local residents reported an abrupt change in the color and clarity of the surface waters of the WB from clear blue to 'cloudy' and 'green' in November 2014, and a subsequent seasonal 'greening' of the lake (Nikl et al., 2016). Although the short-term (3-months) water property

impacts of the MPMC spill have been described by Petticrew et al. (2015) and initial studies on how the spill affected sediment/soils geochemistry and benthic microbial communities have been undertaken (Byrne et al., 2018; Garris et al., 2018; Hatam et al., 2019; Hudson-Edwards et al., 2019), there has not been an investigation into the long-term impact of the spill on the physical limnology of the lake. The influence of the high dissolved solids and suspended sediment loads on density and seasonal mixing processes, the transport and redistribution of suspended sediment in the lake, and the potential for resuspension of waste material from the bed are all unknown, yet these processes are critical to understanding the potential mobilization of contaminants in the water column and their impact on lake ecology.

To complicate matters, in December 2015, to manage site runoff, MPMC was issued a permit to discharge mine-contact water effluents into the WB at depth via a diffuser (MPMC, 2016a). Constraining all factors affecting the long-term water quality of Quesnel Lake, including both the spill and the continued effluent discharge, is of critical importance as its watershed supports substantial recreation, world-renowned resident trout fisheries, and multiple Fraser River Pacific salmon stocks (*Oncorhynchus* spp.) that are vital to indigenous, recreational, and commercial fisheries.

We present over a decade (2006 – 2017) of pre- and post-spill in situ observations to document the impact of the spill and subsequent mining operations on the physical limnology (temperature, conductivity, and turbidity) of Quesnel Lake. Our specific objectives are to: 1) present pre-spill baseline measurements against which post-spill water properties are compared; 2) describe the progression of water property changes from 2014 to 2017 particularly the fate of spill-related suspended sediment; 3) investigate possible sources of and mechanisms for the reported changes to surface water color and clarity; and 4) investigate the impact of effluent discharge from the diffuser on water properties in the WB. The extensive dataset presented here, along with the otherwise undisturbed nature of Quesnel Lake, allow for characterization of the physical dispersal of tailings in an aquatic system to an extent rarely achievable in other spill-impacted water bodies, and provides new insight into physical processes that can drive chronic mobilization and transport of spill materials even in deep lacustrine systems.

2. Site Description

Quesnel Lake is the third deepest lake in North America (mean and maximum depths of 157 and 511 m, respectively; 266 km^2 area; 41.8 km^3 volume; Laval et al., 2008). The lake consists of three narrow arms: the 45 km long West Arm (which includes the WB) extends from the Quesnel River outlet near the community of Likely, BC to the Junction where the lake splits into the North and East Arms (Figure 1). The lake has a hydraulic residence time of 11 yr based on mean annual outflow of the Quesnel River (121 $m^3 s^{-1}$ from 1924-2017), while the shallower WB (mean and maximum depths of 43 m and 113 m, respectively; 23 km^2 area; 1 km^3 volume) has a hydraulic residence time of ~14 weeks. The WB is subject to large amplitude wind-driven internal wave seiching due to wind forcing in the larger Main Basin (Laval et al., 2008). Laval et al. (2008) estimated that during the summer stratified season, internal seiching could exchange 25-30% of the WB hypolimnetic volume over the sill during an upwelling episode, giving a seiche-based exchange residence time for the WB on the order of 6-8 weeks (Laval et al., 2008). The WB was historically dimictic, with near-bottom temperatures varying between 2.5 ºC to 5.5 ºC seasonally, becoming fully isothermal in spring (March-April) and late autumn (November-December) each year (Laval et al., 2012; Petticrew et al., 2015).

Historically, the waters of Quesnel Lake were reportedly clear (average Secchi depths ranging from 8.8 m to 10.2 m between 1981 and 2004; Hume et al., 2005; Nidle et al., 1994; Stockner & Shortreed, 1983), with low ionic concentrations (conductivity of 111-122 µS cm^{-1} estimated from Laval et al., 2012), and low suspended sediment concentrations (turbidity < 1 FTU; Petticrew et al., 2015). The main natural source of suspended sediment to the lake is Niagara Creek whose drainage catchment includes 51 km^2 of glaciated terrain that provides considerable clay-silt loads to the East Arm (Gilbert & Desloges, 2012). The two other main inflows, the Mitchell River in the North Arm, and the Horsefly River in the West Arm east of the sill, have comparatively low sediment loads (Gilbert & Desloges, 2012). As a result, historical sediment accumulation rates in Quesnel Lake were low, varying from 0.2 - 0.7 mm yr^{-1}, with the lowest rates found in the WB and consisting mainly of silts and clays with a mean particle size of ~10 µm (Gilbert & Desloges, 2012).

3. Methods

3.1 Water Column Observations

Water properties in Quesnel Lake were measured between 2006 and 2017 using a Seabird Electronics SBE19plus conductivity-temperature-depth (CTD) profiler equipped with Seapoint optical turbidity and chlorophyll fluorescence sensors. Forty-three pre-spill profiles were collected during seven field campaigns between 2006 and 2012 (Figure 1). Following the spill, repeat CTD profile transects were conducted on a weekly to biweekly basis until December 2017, each survey consisting of ~10 profiles along the length of the West Arm, for a total of 612 post-spill profiles (Figure 1). In addition, transects extending through the West, North and East arms were conducted in May 2007, September 2008, July 2015, and August 2016. No profiles were collected during winter (January-March).

Timeseries of temperature, turbidity, chlorophyll fluorescence, and current velocity were continuously recorded from November 2014 to September 2017 by three moorings deployed in the West Arm. From west to east the moorings were: 1) ADCP1 in 57 m of water near the Quesnel River outlet; 2) M3 in 104 m of water approximately 0.7 km offshore from Hazeltine Creek; and 3) ADCP2 in 64 m of water immediately east of the sill (Figure 1c). Mooring M3 contained 10 thermistors (T-solos, RBR Ltd.) distributed from 2 m to 90 m depth, and one turbidity-chlorophyll fluorescence sensor (Infinity-CLW ACL, JFE Advantech Co. Ltd.) at 5 m. Moorings ADCP1 and ADCP2 each consisted of five thermistors distributed from 2 m to 55 m depth, one turbidity-chlorophyll fluorescence sensor at 5 m depth, and a bottom-mounted upward looking 300 kHz Acoustic Doppler Current Profiler (ADCP, Teledyne RD Instruments).

Nominal sensor accuracies of the profiling and moored instruments were ±0.003 ºC for temperature, ±3 μS cm^{-1} for conductivity, ±0.37 dbar for pressure, ±2% FTUs for turbidity, and ±1% for chlorophyll fluorescence. An issue with the pump on the SBE19plus profiling CTD resulted in larger than nominal errors in temperature (±0.2 ºC) and conductivity (±4 μS cm^{-1}) for profiles collected since 2010, and features <3 m in vertical scale were not fully resolved (Text S1 & Figure S1). Conductivity was referenced to 25 °C and calculated with the LimCond toolbox (Pawlowicz, 2008) using the concentrations of

ionic constituents measured in water samples collected in 2002 (James, 2004; Laval et al., 2012). Note, the values reported in Petticrew et al. (2015) are ~5 μS cm^{-1} higher on average than those reported here owing their use of the EOS-80 calculation (Fofonoff & Millard, 1983). Moored turbidity timeseries data were noisy due to biofouling (associated with a simultaneous rapid increase in chlorophyll fluorescence), therefore, turbidity data were discarded when chlorophyll fluorescence was > 1.5 μg L^{-1}. Offsets in moored turbidity data (maximum offset 0.35 FTU) were corrected using profiler turbidity data as a reference. ADCP velocities were binned to 1 m depth intervals and had an accuracy of 0.5 cm s^{-1}.

To obtain an estimate of the concentration of suspended sediments throughout the water column, the raw ADCP echo intensity data in decibels (dB) were converted to a volumetric backscatter coefficient (Sv in dB referenced to $[4\pi m]^{-1}$) using generic system parameters as presented in Deines (1999). Echo intensity is dependent on several factors, including the type of suspended matter (e.g., plankton, bubbles, and sediment), size, shape, density, and composition (e.g., organics or inorganics) of particles, so Sv provides only a relative estimate of total undifferentiated suspended matter in the water column. However, given the historic low organic concentrations and plankton biomass in Quesnel Lake, we consider Sv a reasonable proxy for the relative abundance of suspended sediment in the water column.

3.2. Remote Sensing Imagery

To investigate anecdotal reports of changes in turbidity and surface water color multiple quasi-true-color Moderate Resolution Imaging Spectroradiometer (MODIS) images (500 m pixel size), were downloaded from NASA Worldview [https://worldview.earthdata.nasa.gov/]. The MODIS corrected reflectance products have gross atmospheric effects (e.g., Rayleigh scattering) removed to create a quasi-true-color images that are only intended for qualitative purposes (http://gis-lab.info/docs/modis_true_color.pdf). For improved visualization of the 2014 autumn turnover water color change, a high resolution (2 m) FormoSat2 image acquired on 11 November 2014 was obtained from Apollo Mapping [https://www.apollomapping.com]. Apollo Mapping created a quasi-true-color image by pansharpening the 8 m multispectral bands to 2 m resolution, merging red (630-690 nm), green (520-600 nm), and blue (450-520 nm) bands in

ENVI software [https://www.harris.com]. All images were finally imported into QGIS [https://qgis.org], cropped, and brightness was manually adjusted for consistency.

3.3. Lake Sediment Cores

To investigate the potential mobilization of spill-related fine particles as a source of water color changes, sediment cores were collected throughout Quesnel Lake between 11 and 18 July 2016. The cores were collected using a mini slo-corer that preserves any unconsolidated layers at the sediment–water interface (Bothner et al., 1998; Law et al., 2008; Milligan & Law, 2013). Here, we present a visual description of four cores that represent the spill impact gradient. The cores were categorized by proximity to the spill inflow, visual lithology, and total metals concentration per Hatam et al., (2019): 1) maximum impact (site C6 in 103 m of water in the main tailings deposit in the center of the WB); 2) low to moderate impact (sites C3 in 51 m and C11 in 53 m of water on the fringes of the WB deposit); and 3) undisturbed (site C18 in 115 m of water in the North Arm) (Figure 1c).

4. Results

4.1. Pre- Versus Post-Spill Water Column Changes

Changes in water properties from 2006 to 2017 are apparent from the timeseries of WB water column profiles and West Arm profile transects (Figures 2 & 3). Prior to the spill (2006-2012), the WB had low conductivity (100-108 μS cm^{-1}), turbidity (<2 FTU) and chlorophyll fluorescence (< 2.5 μg L^{-1}) throughout the water column (Figure 2). WB hypolimnetic temperatures varied between 4ºC and 5ºC, and conductivity and turbidity were nearly uniform at depths >30 m (~107 μS cm^{-1} and <0.5 FTU, respectively). West Arm CTD profile transects showed temperature and conductivity profiles in the Main Basin were similar to the WB prior to the spill (Figure 3), although some spatial variability in turbidity was observed. Pre-spill turbidity was typically <0.5 FTU over all depths at all profiling sites, with the exception of May 2008 and April 2012, when elevated turbidity (2-10 FTU) associated with the Horsefly River plume was observed east of the sill (Figures 2 & 3). Overall, pre-spill water column observations confirm that the waters of Quesnel Lake, and in particular the hypolimnetic waters of the WB, were clear, oligotrophic, and with low dissolved and suspended solids concentrations prior to the spill.

The substantial impact of the spill is readily apparent in the highly elevated hypolimnetic temperature, conductivity, and turbidity values observed in the WB profiles and West Arm transects collected in 2014 post-spill (Figures 2 & 3). The temperature inversion present at depths below 35 m persisted for several months after the spill, but the thermal density anomaly was compensated for by the combined influence of elevated conductivity and total suspended sediment (TSS; estimated from turbidity; see Supplemental Material S2) resulting in a stable water column through to 5 November 2014 (Figure S2). At this time, hypolimnetic conductivity and turbidity ranged from ~110 μS cm^{-1} and ~5 FTU at the base of the surface mixed layer to 150 μS cm^{-1} and to ~90 FTU at the lake bottom, respectively, an indication of spill-related particles settling to the lake bed. Chlorophyll fluorescence remained relatively low (<0.4 μg L^{-1}) in the hypolimnion throughout autumn 2014 (Figure 2), indicating that elevated turbidity in the hypolimnion was associated with suspended sediment and not phytoplankton. The turbidity plume at the base of the thermocline (see also Petticrew et al., 2015) had propagated at least 23 km east of the sill, having a turbidity of 2.25 FTU at the Junction, while a lower turbidity plume appeared to plunge along the bottom of the Main Basin (Figure 3).

Mooring data (Figure 4) show the WB became isothermal by 22 November 2014 which is reasonably consistent with the timing variation observed in previous years, indicating the increased water density caused by elevated dissolved and particulate solids did not substantially influence the timing of turnover. Near-surface turbidity increased rapidly as solids-laden subsurface water was mixed upward, reaching a maximum of almost 10 FTU at 5 m depth at mooring ADCP1 by 22 November 2014 (Figure 4d). The WB then cooled isothermally until reaching the temperature of maximum density in mid-December 2014, thereafter weak inverse thermal stratification was established over winter (surface temperatures were ~1ºC less than bottom temperatures). Near-surface turbidity decreased to 1-1.5 FTU by late February 2015. The WB became isothermal in early March 2015, which coincided with a slight near-surface turbidity increase from 1.25 to 1.75 FTU (Figure 4d), indicative of mixing of turbid deep waters to the surface. As the WB thermally stratified in spring 2015, near-surface turbidity decreased again, to below 1 FTU in April 2015.

Water column profiles from 13 May 2015 (Figures 2, 3 & 4) showed that water properties in the WB were substantially different than the previous autumn. Hypolimnetic temperatures had cooled below 5 ºC, consistent with historical values. Water column conductivity had decreased from >150 μS cm^{-1} to ~110 μS cm^{-1} by spring 2015 throughout the water column and stayed constant for the remainder of the year. Turbidity had also substantially decreased throughout the water column, ranging from 0.5 FTU at the surface to 1.5 FTU at the bottom. Turbidity decreased further during summer 2015, dropping to a minimum of 0.5 FTU at almost all depths by August 2015 (Figure 2). In May 2015, profiling transects along the West Arm showed that WB conductivity and turbidity were elevated by 5 μS cm^{-1} and 0.5 FTU, respectively, above equivalent depths in the Main Basin, yet by August 2015 values were nearly uniform throughout the entire West Arm at 110 μS cm^{-1} and 0.5 FTU, respectively (Figure 3). Remarkably, these observations show that the temperature, conductivity, and turbidity of the entire West Arm, including the WB, had apparently returned close to historic levels by late summer 2015, one year after the spill. This return to pre-spill conditions was temporary, however, as subsequent observations from 2015-2017 showed periods of elevated turbidity and conductivity.

4.2. Post-Spill Seasonal Turbidity Increase (2015-2017)

A key finding from the post-spill observations is a seasonal turbidity increase each spring and autumn in the hypolimnion of the WB. In 2015, 2016, and 2017 the turbidity of the WB was at an annual minimum of approximately 0.5 FTU in late summer (August/September; Figure 2), consistent with pre-spill values. However, in autumn (October/November) each year there was an increase in average WB hypolimnetic turbidity to 1-2.5 FTU (Figures 2, 3 & 5). Turbid hypolimnetic waters were subsequently mixed to the surface during mixis each year, with the moored near-surface turbidity sensors recording up to a 1 FTU increase in turbidity above background (Figure 4). During the subsequent winter, near-surface turbidity either decreased slightly or remained constant, followed by a slight increase during the following spring (March-May) turnover, then a decrease in turbidity to the annual minimum by August. The seasonal turbidity cycle observed in the WB was not apparent east of the sill, where turbidity remained relatively low (<0.5 FTU) from summer 2015 onward (Figure 5).

4.3. West Basin Water Color and Clarity

The increase of surface turbidity in the WB during autumn turnover of 2014 coincided with a distinct water colour change as identified from quasi-true-color satellite imagery (Figure 6). Consistent with all MODIS images available since 2001, the two representative pre-spill images show the entire West Arm appeared dark blue or black and the waters of the WB were visually indistinguishable from those of the Main Basin. Even after the spill, but prior to autumn turnover, the image acquired on 20 September 2014 shows the surface waters were still dark, revealing little evidence of the highly turbid hypolimnetic waters. However, the high resolution FormoSat2 image acquired on 11 November 2014, shows the striking change in reflectance of the WB that occurred as hypolimnetic waters were mixed to the surface – while the Main Basin remained dark blue, the entire WB became a distinct cloudy and bright green color (Figure 6d). The reflectance intensity appeared even stronger in the MODIS image acquired on 15 December 2014 (Figure 6f), close to when recorded near-surface turbidity in the WB peaked between 6-9 FTU (Figure 4), then gradually decreased until it was no longer discernable after April 2015 (Figure 6h-j). Near-surface turbidity remained <1.5 FTU, and generally <1 FTU, after this date, suggesting the green coloration was only visually apparent in the quasi-true-color MODIS imagery when turbidity concentrations were >2 FTU.

4.4. Sources of Suspended Solids

Water column profile transects extending along the West Arm (Figures 3 & 5) and into the East and North Arms (Figure S3) show point sources of turbidity from river plumes, most notably from Niagara Creek in the East Arm. However, in no transects collected since the spill do any of these river plumes extend into the WB, effectively eliminating rivers flowing into the Main Basin as possible sources of the seasonal hypolimnetic turbidity increase in the WB. Several small streams flow directly into the WB, however, most of these have small catchments that drain largely forested landscapes and the historically clear waters of the WB also suggest limited local sediment input. The major exception is the Hazeltine Creek catchment where large swaths were deforested during the spill leaving exposed sediment (Figure 1c). Elevated near-surface turbidity (>5 FTU) was observed near the mouth of Hazeltine Creek in late August 2014 (Petticrew et al., 2015), however restoration efforts along Hazeltine Creek (MPMC, 2016a) seem to have reduced sediment loads as no turbidity

signal >0.2 FTU above background was detected near its mouth from 2015 through 2017 (Figure 3).

Overall, our observations indicate the seasonal turbidity source is local to the WB, appears to originate near the lake bed, and is therefore likely related to mobilization of spill-associated bottom solids. Visual inspection of sediment cores collected in the WB showed an unconsolidated layer of particles existed at the sediment–water interface at sites that were impacted by the spill, a layer that was not present at coring sites further afield (Figure 7). The core from site C18 (undisturbed) in the North Arm showed a distinct sediment–water interface, with only a thin (~1 mm) unconsolidated layer overlying compacted sediment (Figure 7a). In contrast, all cores collected in the WB had a much less distinct sediment–water interface (Fig. 7b-d), and instead showed a 2-3 cm thick unconsolidated layer composed of very fine white-colored particles overlying consolidated natural sediment or tailings material. That the unconsolidated layer was only observed in the WB strongly suggests it was associated with the spill, and if mobile, which it appears to be, suggests it is a possible source for the observed seasonal turbidity signal in the WB.

The flushing of suspended sediment from the WB since the spill, and potentially the mobilization of the unconsolidated bottom layer at the sediment–water interface, could be driven, in part, by baroclinic motions in hydrodynamically active Quesnel Lake. Water velocity timeseries recorded at mooring ADCP2 show depth variable two-way exchange flow over the sill, oscillating with a periodicity between 3 to 6 days, indicating the passage of internal seiches (Figure 8). Current speeds across the sill were often in the range of 50 mm s^{-1} in east or west directions, however eastward outflow speeds reached >150 mm s^{-1} at times (e.g., below 20 m in June-August 2016). The acoustic backscatter record shows high pulses, with peaks up to 25 dB higher than background, indicating roughly 300 times higher scatterer density during these pulses. The timeseries comparing current speed with backscatter intensity at 48 m depth (Figure 8c) reveals the high backscatter peaks were associated with strong outflow velocities suggesting that turbid waters originated in the WB and were advected into the Main Basin, not the reverse. Note that ADCP2 was located at 60 m depth just eastward of the sill in the Main Basin, so these observations are not entirely representative of the conditions within the WB itself.

4.5. Elevated Conductivity in the West Basin

Observations have revealed seasonal anomalies in turbidity from 2015-2017, however, anomalous conductivity values were also observed in the WB in 2016. After returning to near historic values (~110 μS cm^{-1}) from August 2015 to April 2016, conductivity subsequently increased at mid-depths (25-75 m) in the WB during spring and summer 2016, reaching a maximum of 125 μS cm^{-1} at 50 m by mid-September 2016 (Figures 2, 3 & 4; note that there are no profile data available from June-July 2016), up to 15 μS cm^{-1} higher than equivalent depths in the Main Basin (Figure 3). These mid-depth peaks of conductivity were associated with small temperature inversions (visible in temperature profiles from 26 August and 14 September 2016; Figure 2), whose destabilizing effect was compensated by elevated conductivity (Figure S2), yet were not associated with any notable turbidity signal. The mid-depth conductivity maximum appeared to be mixed over the water column during autumn turnover 2016, varying from ~110 μS cm^{-1} at the surface to 115 μS cm^{-1} near the bottom on 1 December 2016 (Figure 2). Subsequently, conductivity remained relatively homogenous and constant between 109 and 112 μS cm^{-1} throughout the West Arm during 2017. We suggest, and discuss further below, that the elevated conductivity in 2016 was, in part, associated with MPMC's discharge of mine-related effluent into the WB via the diffuser.

5. Discussion

5.1. Impact and Fate of Spill Material

We have presented the first multiyear observations of the impact of a catastrophic tailings spill on the physical limnology of a deep, oligotrophic and relatively pristine lake. Our observations have shown that the MPMC tailings spill resulted in a massive transformation of water properties within the WB, the impact initially confined to the hypolimnion. Given the increased density of hypolimnetic waters of the WB due to elevated dissolved and suspended solids following the spill, it was initially uncertain as to whether or not the WB would mix to the bottom during autumn overturn 2014, yet our mooring records show that the WB did become isothermal to at least 94 m depth by 22 November 2014. This is perhaps unsurprising in hindsight, given the increase in density of the contaminated hypolimnion was only on the order of 0.1 kg m^{-3}, which is an order of magnitude smaller than

the ~1 kg m^{-3} density difference overcome each year during seasonal mixing across the thermocline (Figure S2).

The true scale of the spill and its impact on the lake only became visually apparent at the surface when contaminated hypolimnetic waters were mixed throughout the water column, turning the lake bright green. Although several factors determine water color, including the concentrations of phytoplankton and colored dissolved organic matter (Wetzel, 2001), we suggest the explanation for the observed 'greening' of Quesnel Lake post-spill is the presence of small inorganic particles in low concentrations in the water column (c.a. Aas & Bogen, 1988). The presence of fine particles including suspended clays (<2 μm) and silts (2-63 μm) at low concentrations (<20 mg L^{-1}) can shift the reflectance maximum of water toward green wavelengths (Aas & Bogen, 1988). Petticrew et al. (2015) showed the median particle size distribution in the hypolimnion several weeks after the spill in 2014 was 1 μm, and the concentration of suspended sediment in Quesnel River outflow ranged between 0.5 – 5 mg L^{-1}, with the higher concentrations observed during 2014 autumn turnover after the spill (unpublished data). These observations suggest that the green coloration could have been due to the mixing of small (~1 μm), low-concentration (<5 mg L^{-1}) of spill-related inorganic particulates to the surface during turnover.

The WB bore the main impact of the spill, however CTD transects revealed that by early November 2014, spill-related material had been carried at least 30 km eastward to the Junction, and likely beyond by the end of 2014 (Figure 3). The subsurface turbidity plume at the base of the thermocline advanced ~10 km between Station 2 and 88 over 30 days in October-November 2014, giving an average propagation speed of ~0.4 cm s^{-1}, less than half the 1 cm s^{-1} plume speed estimated by Petticrew et al. (2015) between 6 August to 2 October 2014. Taking a range between 0.1 and 1 cm s^{-1}, we estimate the plume could have advanced between 1 km to 36 km past the Junction in the 2-6 weeks before the upper 200 m of the Main Basin became isothermal. Turbidity sensors on two additional moorings deployed in North and East Arms (7 km and 10 km past the Junction, respectively) each recorded a small but discernable 0.1 FTU turbidity increase at ~30 m depth above background (0.3-0.4 FTU) in late November 2014 (Figure S4). These observations are further evidence that the spill-

related plume had propagated throughout all arms of Quesnel Lake prior to autumn turnover in 2014.

5.2. West Basin Seasonal Turbidity Increase

Our evidence indicates the post-spill seasonal turbidity increase in the hypolimnion of the WB was due to physical mobilization of a spill-related unconsolidated layer at the sediment–water interface. However, the precipitation of chemicals, such as iron (Fe) and calcium (Ca) salts or minerals, in the water column as an alternate explanation for the turbidity signal was also considered given the influx of dissolved and solid metals during the spill (MPMC, 2016a). Analysis of available chemical data published in MPMC quarterly water quality reports (BC MoE, 2019), indicates that while the redox state of the lake is favorable for the formation of Fe_2O_3 (iron oxide, likely ferric oxy-hydroxides; Figure S5), the concentration of total iron in the WB is very low (mostly below the 0.03 mg L^{-1} detection limit of the measurement technique) indicating any role it has in the seasonal turbidity increase is relatively minor. The availability of data limits analysis of the possibility of the formation of calcium carbonate and other chemical precipitates, so their role remains uncertain, however, physical mobilization seems the likely dominant source of turbidity.

There are several lines of evidence to support the physical mobilization of spill-related material hypothesis: 1) our observations indicate the turbidity source is local to the WB hypolimnion; 2) the turbidity signal is initially only present at depths greater than 35 m which is consistent with where the initial load of spill-related sediments on the lake bed was highest (Potts et al., 2015); and 3) the presence of a turbid unconsolidated layer associated with tailings deposits in the WB provides a possible source for the particles. The unconsolidated layer in core C11 was between 2-3 cm thick and had a turbidity between 500-1000 FTU from preliminary laboratory analysis (data not shown). If this layer, which is present in each WB core, was distributed over an area between 12-25 km^2 in the WB and was completely mixed over the full water column at turnover, this would equate to an average water column turbidity increase in the range of 0.1-0.7 FTU, which is broadly consistent with the observed turbidity increase of 0.5 to 1.0 FTU between summer and autumn each year, supporting the mobilization hypothesis.

Mobilization of unconsolidated material at the sediment–water interface requires a mechanism to generate turbulence near the lake bed and mix the material into the water column of which there are many (e.g., see Lawrence et al., 2016). The main mechanisms are related to the development of a benthic boundary layer forced by shear stress from baroclinic motions (Gloor et al., 1994; Imboden & Wüest, 1995; Shteinman et al., 1997) or downwards propagation through a homogenous water column of surface generated turbulence (i.e., wind stirring or convection). In littoral zones and shallow lakes surface generated turbulence is important (e.g., Marvin et al., 2004, 2007; Matisoff & Carson, 2014), however, because the WB was still thermally stratified when hypolimnetic turbidity started to increase in autumn of each year, and is very deep, downward propagation of surface processes as the cause is unlikely. Observations of enhanced near-bottom turbulence induced by breaking internal waves are well established in the coastal ocean (e.g., Boegman & Stastna, 2019, Klymack & Moum, 2003, and references therein), have commonly been observed in lakes (e.g., Bouffard et al., 2012; Farmer, 1978), with some evidence of associated sediment resuspension (Austin, 2013; Hawley, 2004; Valipour et al., 2017). Even in 100 m deep Lake Michigan current speeds in excess of 13 cm s^{-1} have been reported above the bottom with sufficient energy to remobilize the unconsolidated floc from the sediment–water interface (Saylor & Miller, 1988). This indicates that the large internal seiche motions in the WB of Quesnel Lake could be driving resuspension of mine-associated materials to the water column.

The relation between wind forcing and baroclinic response in Quesnel Lake is complicated by topography (Thompson et al., 2020) and lake geometry (Brenner & Laval, 2018), but the unusually large (for a water body of its size) regular oscillations in the WB shown in the mooring and ADCP data are likely baroclinic responses to wind forcing set up in the larger Main Basin of Quesnel Lake (Figure 8; Laval et al., 2008). The summertime, basin-wide, east-to-west, fundamental seiche period (T_i) of Quesnel Lake is estimated at 6 days (Laval et al., 2008), thus wind events must continue for at least 1.5 days (i.e., $T_i/4$) at a consistent speed and direction in order to excite this mode of seiche (Spigel & Imberger, 1980; Stevens & Imberger, 1996). Between 2016 and 2018, the frequency of 80th percentile mean wind stress events (>12.5 m s^{-2}) that lasted for a minimum of 36 hrs had the highest occurrence in spring and autumn (Thompson et al., 2020). The amplitude of internal waves in the WB are historically largest during autumn during weakening water column stratification (Laval et al., 2008). In autumn of 2015, the increase in hypolimnetic turbidity coincided with

a period of strong internal wave activity (Figure 8). Thermistor records from the center of the WB show that the increase in turbidity below the thermocline in September and October of 2015 and 2016 coincided with initiation of large amplitude temperature fluctuations and increased heating rate below the seasonally deepening surface mixed layer (e.g., the thermistor at 29 m depth in Figure 9), that were due to increased vertical heat flux driven by increased turbulence within the thermocline. Hypolimnetic turbidity increased each year during autumn from the bottom upward as the heating rate of hypolimnetic water increased and the mixed layer deepened, until a fully isothermal state was reached in late November of 2015 and 2016 (Figure 9). In summary, we suggest that mobilization of particles from the unconsolidated layer is initiated by shear forces at the bed generated by baroclinic motions *combined* with surface layer deepening beyond ~30 m depth.

Maintenance of elevated turbidity after turnover appears to require an unstratified water column with active surface-driven mixing (i.e., no ice cover). Turbidity remained elevated all winter of 2015/16 while the lake was isothermal, while during the winter of 2016/17 near-surface turbidity dropped back to summer background levels during January-March when the lake was ice-covered and inverse stratification was present. These observations suggest that surface driven turbulence is sufficient to maintain suspension of bed material, while inverse stratification and ice-cover suppress turbulence, allowing suspended particles to settle back to the bed. The highest near-surface turbidity between 2015-2017 was observed in spring 2017, three years after the spill, indicating this is an on-going issue for Quesnel Lake.

Our findings indicate that where the bathymetry, geometry, and atmospheric forcing of a lake induce large internal seiche motions, even deeply (i.e., ~100 m) submerged bottom sediments may be prone to re-suspension, depending on the composition of the sediments. Where full-depth mixing occurs, as is the case in the WB, this could lead to the exchange of dissolved and particulate constituents, including tailings-associated contaminants, between the upper and lower water column, with associated influences on lake biogeochemistry, photosynthetic rates, and ecology (Frechette et al., 1989; Gloor et al., 1994; Lou et al., 2000). In situ studies have shown that bottom shear stresses in small (ten Hulscher et al. 1992; de Vicente et al. 2010; Wang et al. 2017) and very large lakes, such as Lake Winnipeg (Matisoff

et al., 2017) and the Laurentian Great Lakes (Marvin et al., 2004, 2007; Schneider et al., 2002), can cause sediment-vectored transport of heavy metals, hydrophobic organopollutants, and nutrients from sediment to the water column in masses that contribute significantly to total lake budgets. Preliminary data indicates seasonally high total copper concentrations in suspended sediment in Quesnel River measured at the Quesnel River Research Centre (QRRC; Fig. 1) in spring and autumn from 2015 through 2019 (unpublished data), which is of concern as exposure to elevated copper concentrations can negatively affect aquatic life. Chronic exposure to elevated copper concentrations in fish can lead to growth reduction, reduced reproductive rates, impaired olfaction, decreased survival, altered swim performance, and avoidance behavior which can reduce the overall extent and diversity of available habitat, resulting in population decline (BC MoE, 2019 and references therein). From a fisheries perspective, this could have significant ecosystem and economic implications given that, in dominant years, >1 million sockeye salmon (*Oncorhynchus nerka*) migrate through Quesnel Lake to the Horsefly and Mitchell rivers to spawn, and the lake itself provides rearing habitat for large numbers (10^6–10^8) of juvenile sockeye salmon (Crossin et al., 2004; Hume et al., 1996; Levy et al., 1991; Lilja et al., 2008). The possibility that seiche-driven resuspension of spill material from Quesnel Lake is mobilizing contaminants into the water column and the Quesnel River is therefore a critical area of ongoing investigation.

5.3. West Basin Elevated Conductivity

The observed timing of elevated conductivity in the WB at mid-depths in 2016 can be explained, in part, by changes to discharge of waste water from the MPMC mine site. In late 2015, to draw-down water levels on the mine site, MPMC was granted permission, for the first time, to discharge mine contact water into the WB via twin two-port diffusers installed at 45 and 50 m depth offshore of the mouth of Hazeltine Creek; the discharging effluent had a high mean conductivity of 1196 ± 60 µS cm^{-1} during 2016 and 2017 (MPMC, 2017). Discharge rates increased during spring 2016 and remained high, with a total volume of 6.71 Mm^3 discharged in 2016. In 2017, the total volume discharged decreased substantially to 2.02 Mm^3, owing, in part, to stabilization of mine site water levels, but also the result of extended periods (e.g., 30 March - 6 June, 10-27 July, and 1 October - 31 December 2017) when discharge ceased completely to comply with permit requirements (MPMC, 2018). That mine discharge reached a maximum in mid to late 2016 and decreased thereafter may explain the elevated conductivity observed in the WB in summer 2016 when the discharge plume was

contained as an interflow below the seasonal thermocline. In 2017, the lack of an observable discharge plume was likely due to lower total mine discharge, with minimal (14% of annual total) discharge occurring during summer stratification, and a two-month gap in CTD profiles from June to August 2017. Although the high conductivity of the discharge effluent appears to have episodically altered the conductivity of the WB, other possible sources, including contaminated runoff from the Hazeltine Creek watershed are under investigation. The impact of elevated dissolved solids in the WB on the physical and biogeochemical processes in the lake are as yet unknown.

5.4. Context and Implications

The magnitude of the Mount Polley mine tailings spill, by volume released, has been exceeded only by the 2015 Samarco mine failure in Brazil (WISE, 2020). The sheer scale of the Samarco disaster was visibly apparent as the surface tailings plume propagated hundreds of kilometers downriver and spread out into the Atlantic Ocean (Fernandes et al., 2016). In contrast, the bulk of the Mount Polley tailings plume disappeared from view when it plunged to the bottom of Quesnel Lake, to some extent masking the scale of the spill. In marked contrast to many other tailings spills which have impacted vast downstream aquatic areas (Kossoff et al., 2014), the thermal stratification and semi-isolated geometry of the WB contained the majority the spill to a relatively small area (~12 km^2), meaning that the WB of Quesnel Lake is likely to bear the brunt of any associated ecological consequences. The waste from the Mount Polley spill was less acutely toxic than other tailings dam failures (e.g., the 2000 Baia Mare cyanide spill in Romania, which killed an estimated 1240 tonnes of fish along the Tisa and Danube Rivers; Lásló, 2006; Macklin et al., 2003; Soldan et al., 2000), however heavy metals in the tailings sediments remain a concern for long-term chronic exposure. Resuspension of contaminants is a concern in many shallow riverine systems impacted by spills (Kossoff et al., 2014, and references therein), and our results indicate that it is also a possibility in deep lakes depending on lake hydrodynamics. Although the exact mechanism of internal wave-driven resuspension in Quesnel Lake remains unclear (e.g., turbulence at the bed from basin-scale seiches, or topographically induced breaking internal waves over the sill, etc.), it is apparent that an understanding of lake hydrodynamics is critical to understanding the fate and transport of contaminated sediments. These processes are highly seasonal and thus aquatic monitoring strategies must account for these temporal variations. The results of this study indicate that investigation of lake physics is a critical

component of any multidisciplinary effort to understand possible impacts of tailings spills on the chemistry and biology of impacted lakes.

6. Conclusions

Eleven years of physical limnology data demonstrate the impact the August 2014 MPMC tailings spill had on the waters of Quesnel Lake. Although the massive inflow of debris was initially contained below the epilimnion, and its impact not readily visible at the surface, vertical mixing during autumn 2014 turnover brought spill event-related material back to the surface, turning the lake bright green, a change readily visible in satellite imagery. Despite the magnitude of the spill, most of the excess heat, dissolved and suspended solids in the water column were flushed from the WB, or settled, over winter 2014/15, and from the perspective of the physical water properties alone, it appeared the lake had returned to a near pre-spill state 12 months following the breach. However, during each spring and autumn overturn since 2015, turbidity increased in the hypolimnion of the WB, and we argue that this is associated with the mobilization of particles from an unconsolidated layer of spill-related sediments at the lake bed. Mobilization of this layer is likely driven by turbulence associated with internal seiching and seasonal mixed layer deepening. These seasonally mobilized particles then remain in suspension until the lake restratifies, at which point turbidity decreases, due to a combination of particle settling and export out of the WB. The impact of the seasonally elevated turbidity on the ecology of the lake, the possibility for sediment-associated mobilization of contaminants, and the persistence of this phenomenon in future years are critical topics requiring further investigation.

Discharge of effluent from the mine also appears to alter the water properties of the WB, as seen by increased conductivity in the WB. Discharge rates in 2018 increased compared to 2017 and as of September 2018 the total cumulative volume of effluent discharged into the WB since 2015 was 10.8 Mm^3 (MPMC, 2018), an amount approaching that of the catastrophic 2014 spill. Continued monitoring of water properties in Quesnel Lake is therefore critical to understanding the long term impacts of the spill through seasonal mobilization of spill event-related sediment, and the ongoing impacts of continued mine effluent discharge. Long term, multidisciplinary study is required not only to understand the

long term impacts on the Quesnel Lake ecosystem, but also to serve as a guide in the regulation of mine discharge into lakes worldwide. Given the unfortunate likelihood of future tailings dam failures (Owen et al., 2020), the need to understand the potential impact of catastrophic tailings spills on waterbodies, including deep lakes, remains a high priority.

Acknowledgments, Samples, and Data

This work was primarily supported by Environment and Climate Change Canada's Environmental Damages Fund (Project:1000371667-EDF-CA-2015/002). In addition, Laval's research was supported by the NSERC Discovery and Discovery Accelerator programs, as well as the UBC Department of Civil Engineering Flood Fund. The authors thank Samuel Brenner, Laszlo Enyedy, Caitlin Langford, Leo Nodwell-Laval, Judith Pringle, Natasha Wallbrink, and Trevor Warkentin for research assistance. The comments and suggestions of improvements by Erich Hester and two anonymous reviewers are gratefully acknowledged.

The dataset used in this study is available online at the Scholars Portal Dataverse: https://dataverse.scholarsportal.info/dataset.xhtml?persistentId=doi:10.5683/SP2/BIBUBF

References

Aas, E., & Bogen, J. (1988). Colors of glacier water. *Water Resources Research, 24*, 561-565. https://doi.org/10.1029/WR024i004p00561

Austin, J. (2013). Observations of near-inertial energy in Lake Superior. *Limnology and Oceanography, 58*, 715-728. https://doi.org/10.4319/ lo.2013.58.2.0715

Azam, S., & Li, Q. (2010). Tailings dam failures: a review of the last one hundred years. *Geotechnical News, 24*(4), 50-54.

Babić-Mladenović, M., Varga, S., & Damjanović, M. (2002). The pollution of the 'Iron Gate' reservoir. In J. Vujic (Ed.). *Proceedings of the First International Conference on Environmental Recovery of Yugoslavia*, 852 pp. Yugoslavia: Institute of Nuclear Sciences VINCA. (ISBN 86-7306-054-0)

BC MoE. (2017). *British Columbia working water quality guidelines: aquatic life, wildlife & agriculture*. British Columbia Ministry of Environment, Water Protection & Sustainability Branch, Victoria, BC, Canada**,** 37 pp. Retrieved from https://www2.gov.bc.ca/assets/gov/environment/air-land-water/water/waterquality/water-quality-guidelines/bc_env_working_water_quality_guidelines.pdf (accessed 17 Apr. 2020)

BC MoE. (2019). *Copper water quality guideline for the protection of freshwater aquatic life: technical report*. Ministry of Environment & Climate Change Strategy, Water Protection and Sustainability Branch, Victoria, BC, Canada**,** 66 pp. Retrieved from https://www2.gov.bc.ca/assets/gov/environment/air-land-water/water/waterquality/water-quality-guidelines/approved-wqgs/copper/bc_copper_wqg_aquatic_life_technical_report.pdf (accessed 17 Apr. 2020)

Boegman, L., & Stastna, M. (2019). Sediment resuspension and transport by internal solitary waves. *Annual Review of Fluid Mechanics, 51*, 129-154. https://doi.org/10.1146/annurev-fluid-122316-045049

Bookstrom, A. A., Box, S. E., Campbell, J. K., Foster, K. I., & Jackson, B. L. (2001). *Lead-rich sediments, Coeur d'Alene River valley, Idaho: area, volume, tonnage, and lead content*. United States Geological Survey, Department of Interior, Open-File report 01-140. Menlo Park, CA: Retrieved from https://pubs.usgs.gov/of/2001/of01-140/of01-140.pdf (accessed Apr. 7, 2020)

Bothner, M. H., Buchholtz ten Brink, M., & Manheim, F. T. (1998). Metal concentrations in surficial sediments of Boston Harbor − changes with time. *Environmental Research, 45*(2), 127-155. https://doi.org/10.1016/S0141-1136(97)00027-5

Bouffard, D., Boegman, L., & Rao, Y. R. (2012). Poincare wave-induced mixing in a large lake. *Limnology and Oceanography, 57,* 1201-1216. https://doi.org/10.4319/lo.2012.57.4.1201

Brenner, S. D., & Laval, B. E. (2018). Seiche modes in multi-armed lakes. *Limnology and Oceanography, 63,* 2717-2726. https://doi.org/10.1002/lno.11001

Byrne, P., Hudson-Edwards, K. A., Bird, G., Macklin, M. G., Brewer, P. A., Williams, R. D., & Jamieson, H. E. (2018). Water quality impacts and river system recovery following the 2014 Mount Polley mine tailings dam spill, British Columbia, Canada. *Applied Geochemistry*, *91*, 64-74. https://doi.org/10.1016/j.apgeochem.2018.01.012

Crossin, G. T., Hinch, S. G., Farrell, A. P., Higgs, D. A., Lotto, A. G., Oakes, J. D., & Healey, M. C. (2004), Energetics and morphology of sockeye salmon: effects of upriver migratory distance and elevation. *Journal of Fish Biology*, *65*, 788-810. https://doi.org/10.1111/j.0022-1112.2004.00486.x

Crossin, G. T., Hinch, S. G., Cooke, S. J., Welch, D. W., Batten, S. D., Patterson, D. A., van der Kraak, G., Shrimpton, J. M., & Farrell, A. P. (2007). Behaviour and physiology of sockeye salmon homing through coastal waters to a natal river. *Marine Biology*, *152*, 905-918. https://doi.org/10.1007/s00227-007-0741-x

Davies, M. P. (2001). Impounded mine tailings: what are the failures telling us? *CIM Bulletin*, *94*, 94, 53-59.

Davies, M. P. (2002). Tailings impoundment failures: are geotechnical engineers listening? *Waste Geotechnics*, *20*, 1-36.

Deines, K. L. (1999). *Backscatter estimation using broadband acoustic Doppler current profilers*. Proceedings of the IEEE Sixth Working Conference on Current Measurement (Cat. No.99CH36331), San Diego, CA, USA, pp. 249-253.https://doi.org/10.1109/CCM.1999.755249

de Vicente, I., Cruz-Pizarro, L., & Rueda, F. J. (2010). Sediment resuspension in two adjacent shallow coastal lakes: controlling factors and consequences on phosphate dynamics. *Aquatic Science*, *72*, 21-31. https://doi.org/10.1007/s00027-009-0107-1

Eadie, B. J., Vanderploeg, H. A., Robbins, J. A., & Bell, G. L. (1990). Significance of sediment resuspension and particle settling. In M. M. Tilzer & C. Serruya (Eds.) *Large lakes*. Brock/Springer Series in Contemporary Bioscience. Springer, Berlin, Heidelberg. https://doi.org/10.1007/978-3-642-84077-7_10

Farmer, D. M. (1978). Observations of long nonlinear internal waves in a lake. *Journal of Physical Oceanography*, *8*, 63-73. https://doi.org/10.1175/ 1520-0485(1978)008 < 0063:OOLNIW>2.0.CO;2

Fofonoff, N. P., & Millard, R. C. (1983). Algorithms for computation of fundamental properties of seawater. *UNESCO Technical Papers in Marine Science*, *44*, 53 pp.

Fonseca do Carmo, F., Kamino, L. H. Y., Tobias, R. (Jr.), de Campos, I. C., Fonseca do Carmo, F., Silvino, G., Junio da Silva de Castro, K., Mauro, M. L., Rodrigues, N. U. A., Paulo d Souza Miranda, M., & Pinto, C. E. F. (2017). Fundão tailings dam failures: the environment tragedy of the largest technological disaster of Brazilian mining in global context. *Perspectives in Ecology and Conservation*, *15*(3), 145-151. https://doi.org/10.1016/j.pecon.2017.06.002.

Frechette, M., Butman, C. A., & Geyer, W. R. (1989). The importance of boundary-layer flows in supplying phytoplankton to the benthic suspension feeder, *Mytilus edulis* L. *Limnology and Oceanography*, *34*, 19-36. https://doi.org/10.4319/lo.1989.34.1.0019

Garris, H. W., Baldwin, S. A., Taylor, J., Gurr, D. B., Denesiuk, D. R., Van Hamme, J. D., & Fraser, L. H. (2018). Short-term microbial effects of a large-scale mine-tailing storage facility collapse on the local natural environment. *PLoS ONE*, *13*(4), https://doi.org/ 10.1371/journal.pone.0196032

Gilbert, R., & Desloges, J. R. (2012). Late glacial and Holocene sedimentary environments of Quesnel Lake, British Columbia. *Geomorphology*, *179*, 186-196. https://doi.org/10.1016/j.geomorph.2012.08.010

Gloor, M., Wüest, M. G. A., & Münnich, M. (1994). Benthic boundary mixing and resuspension induced by internal seiches. *Hydrobiologia*, *284*, 59-68. https://doi.org/10.1007/BF00005731

Golder Associates (2017). *Mount Polley rehabilitation and remediation strategy: ecological risk assessment*. Prepared for Mount Polley Mining Corporation, 15 December 2017. 273 p. Retrieved from https://www2.gov.bc.ca/gov/content/environment/air-land-

water/spills-environmental-emergencies/spill-incidents/past-spill-incidents/mt-polley/mount-polley-key-information (Accessed 11 June 2019)

Hatam, I, Petticrew, E. L., French, T. D., Owens, P. N., Laval, B., & Baldwin, S.A. (2019). The bacterial community of Quesnel Lake sediments impacted by a catastrophic mine tailings spill differ in composition from those at undisturbed locations – two years post-spill. *Scientific Reports, 9*, 2705. https://doi:10.1038/s41598-019-38909-9

Hawley, N. (2004). Response of the benthic nepheloid layer to near-inertial internal waves in southern Lake Michigan. *Journal of Geophysical Research, 109*, C04007. https://doi.org/10.1029/2003JC002128

Hudson-Edwards, K. A., Macklin, M. G., Jamieson, H. E., Brewer, P. A., Coulthard, T. J., Howard, A. J., & Turner, J. N. (2003). The impact of tailings dam spills and clean-up operations on sediment and water quality in river systems: the Ríos Agrio–Guadiamar, Aznanalcóllar, Spain. *Applied Geochemistry*, *18*, 221-239. https://doi.org/10.1016/S0883-2927(02)00122-1

Hume, J., Shortreed, K., & Whitehouse, T. (2005). *Sockeye fry, smolt, and nursery lake monitoring of Quesnel and Shuswap lakes in 2004*. Retrieved from https://www.unbc.ca/sites/default/files/sections/quesnel-river-research-centre/frp3hume.pdf

Imboden, D. M., & Wüest, A. (1995). Mixing mechanisms in lakes. In A. Lerman, D.M. Imboden & J.R. Gat (Eds.), *Physics and chemistry of lakes*, pp. 83-138, Springer, New York and Heidelberg. https://doi:10.1007/978-3-642-85132-2_4

Ishihara, K., Ueno, K., Yamada, S., Yasuda, S., & Yoneoka, T. (2015). Breach of a tailings dam in the 2011 earthquake in Japan. *Soil Dynamics and Earthquake Engineering, 68*, 3-22. https://doi.org/10.1016/j.soildyn.2014.10.010

James, C. (2004). *Identifying mixing processes in CTD profiles from Quesnel Lake using a lake-specific equation of state*. Master of Science Thesis, University of British Columbia, Vancouver, BC, Canada. Retrieved from https://open.library.ubc.ca/collections/ubctheses/831/items/1.0063438

Klymak, J. M., & Moum, J. N. (2003). Internal solitary waves of elevation advancing on a shoaling shelf. *Geophysical Research Letters*, *30*, 2045-2049. https://doi.org/10.1029/2003GL017706

Kossoff, D., Dubbin, W. E., Alfredsson, M., Edwards, S. J., Macklin, M. G., & Hudson-Edwards, K. A. (2014). Mine tailings dams: characteristics, failure, environmental impacts, and remediation. *Applied Geochemistry*, *51*, 229-245. https://doi.org/10.1016/j.apgeochem.2014.09.010

Kraft, C., von Tümpling, W., & Zachmann, D. W. (2006). The effects of mining in northern Romania on the heavy metal distribution in sediments of the rivers Szamos and Tisza (Hungary). *Acta Hydrochimica et Hydrobiologica, 34*, 257-264. https://doi.org/10.1002/aheh.200400622

Lásló, F. 2006. Lessons learned from the cyanide and heavy metal accidental water pollution in the Tisa River basin in the year 2000. In G. Dura & F. Simeonova (Eds.), *Management of intentional and accidental water pollution*. NATO Security Through Science Series. Springer, Dordrecht. pp. 43-50. https://doi.org/10.1007/1-4020-4800-9_4

Laval, B. E., Morrison, J., Potts, D., Carmack, E., Vagle, S., James, C., McLaughlin, F. A., & Forman, M. (2008). Wind-driven summertime upwelling in a fjord-type lake and its impact on downstream river conditions: Quesnel Lake and River, British Columbia, Canada. *Journal of Great Lakes Research, 34*, 189-203. https://doi.org/10.3394/0380-1330(2008)34[189:WSUIAF]2.0.CO;2

Laval, B. E., Vagle, S., Potts, D., Morrison, J., Sentlinger, G., James, C., McLaughlin, F., & Carmack, E. C. (2012). The joint effects of thermal, riverine and wind forcing on temperate fjord lakes, *Journal of Great Lakes Research, 38*, 540-549.

https://doi.org/10.1016/j.jglr.2012.06.007

Law, B. A., Hill, P. S., Milligan, T. G., Curran, K. J., Wiberg, P. L., & Wheatcroft, R. A. (2008). Size sorting of fine-grained sediments during erosion: results from the western Gulf of Lions. *Continental Shelf Research, 28*, 1935-1946. https://doi.org/10.1016/j.csr.2007.11.006

Lawrence, G. A., Tedford, E. W., & Pieters, R. (2016). Suspended solids in an end pit lake: potential mixing mechanisms. *Canadian Journal of Civil Engineering, 43*, 211-217. https://doi.org/10.1139/cjce-2015-0381

Leppänen, J., Weckström, J., & Korhola, A. (2017). Multiple mining impacts induce widespread changes in ecosystem dynamics in a boreal lake. *Scientific Reports, 7*, 10581. https://doi.org/10.1038/s41598-017-11421-8.

Levy, D. A., Johnson, R. L., & Hume, J.M. (1991). Shifts in fish vertical distribution in response to an internal seiche in a stratified lake. *Limnology and Oceanography, 36,* 187-192. https://doi.org/10.4319/lo.1991.36.1.0187

Lilja, J., Ridley, T., Cronkite, G. M. W., Enzenhofer, H. J., & Holmes, J. A. (2008). Optimizing sampling effort within a systematic design for estimating abundant escapement of sockeye salmon (*Oncorhynchus nerka*) in their natal river. *Fisheries Research, 90,* 118-127. https://doi.org/10.1016/j.fishres.2007.10.002

Lou, J., Schwab, D. J., Beletsky, D., & Hawley, N. (2000). A model of sediment resuspension and transport dynamics in southern Lake Michigan. *Journal of Geophysical Research: Oceans, 105,* 6591-6610. https://doi.org/10.1029/1999JC900325

Lucas, C. (2001). The Baia Mare and Baia Borsa accidents: cases of severe transboundary water pollution. *Environmental Policy and Law, 31,* 106-111.

Macklin, M. G., Brewer, P. A., Balteanu, D., Coulthard, T. J., Driga, B., Howard, A. J., & Zaharia, S. (2003). The long term fate and environmental significance of contaminant metals released by the January and March 2000 mining tailings dam failures in Maramureș¸ County, upper Tisa Basin, Romania. *Applied Geochemistry, 18,* 241-257. https://doi.org/10.1016/S0883-2927(02)00123-3

Magris, R. A., Marta-Almeida, M., Monteiro, J. A., & Ban, N. (2019). A modelling approach to assess the impact of land mining on marine biodiversity: assessment in coastal catchments experiencing catastrophic events (SW Brazil). *Science of the Total Environment, 659,* 828-840. https://doi.org/10.1016/j.scitotenv.2018.12.238.

Marvin, C. H., Sverko, E., Charlton, M. N., Thiessen, P. A. L., & Painter, S. (2004). Contaminants associated with suspended sediments in Lakes Erie and Ontario, 1997-2000. *Journal of Great Lakes Research, 30*(2), 277-286. https://doi.org/10.1016/S0380-1330(04)70345-7.

Marvin, C., Charlton, M., Milne, J., Thiessen, L., Schachtschneider, J., Sardella, G., & Sverko, E. (2007). Metals associated with suspended sediments in Lakes Erie and Ontario, 2000-2002. *Environmental Monitoring and Assessment, 130,* 149-161. https://doi.org/10.1007/s10661-006-9385-4

Matisoff, G., & Carson, M. L. (2014). Sediment resuspension in the Lake Erie nearshore. *Journal of Great Lakes Research*, *40*, 532-540. https://doi.org/10.1016/j.jglr.2014.02.001

Matisoff, G., Watson, S. B., Guo, J., Duewiger, A., & Steely, R. (2017). Sediment and nutrient distribution and resuspension in Lake Winnipeg. *Science of the Total Environment*, *575*, 173-186. https://doi.org/10.1016/j.scitotenv.2016.09.227

Milligan, T. G., & Law, B. A. (2013). Contaminants at the sediment-water interface: implications for environment impact assessment and effects monitoring. *Environmental Science and Technology*, *47*, 5828-5834. https://doi.org/10.1021/es3031352

Moncur, M. C., Ptacek, C. J., Blowes, D. W., & Jambor, J. L. (2006). Spatial variations in water composition at a northern Canadian lake impacted by mine drainage. *Applied Geochemistry*, *21*(10), 1799-1817. https://doi.org/10.1016/j.apgeochem.2006.06.016.

MPMC. (2015). *Post-event environmental impact assessment report –key findings report*. Prepared for British Columbia Ministry of Environment, 5 June 2015. Retrieved from https://imperialmetals.com/our-operations/mount-polley-mine/mount-polley-updates

MPMC. (2016a*). Mount Polley mine tailings storage facility, perimeter embankment breach update report: post-event environmental impact assessment report*. Prepared for British Columbia Ministry of Environment, 3 June 2016. Retrieved from https://imperialmetals.com/our-operations/mount-polley-mine/mount-polley-updates

MPMC. (2016b). *Mount Polley Mining Corporation 2016 annual discharge plan*. Prepared for British Columbia Ministry of Environment, 16 June 2016. Retrieved from https://imperialmetals.com/our-operations/mount-polley-mine/mount-polley-updates

MPMC. (2017). *2016 annual environmental and reclamation report for the Mount Polley Mine*. Prepared for British Columbia Ministry of Environment, 31 March 2017. Retrieved from https://imperialmetals.com/our-operations/mount-polley-mine/mount-polley-updates

MPMC. (2018). *Third quarter 2018 report for permit 11678*. Prepared for British Columbia Ministry of Environment and Climate Change Strategy, 7 November 2018. Retrieved from https://imperialmetals.com/our-operations/mount-polley-mine/mount-polley-updates

Mudd, G. M. (2007). Global trends in gold mining: towards quantifying environmental and resource sustainability. *Resource Policy*, *32*(1), 42-56. https://doi.org/10.1016/j.resourpol.2007.05.002.x.

Nidle, B. H., Shortreed, K. S., & Masuda, K. V. (1994). Limnological data from the 1985-1990 study of Quesnel Lake. *Canadian Data Report of Fisheries and Aquatic Sciences*, *940*, 82 p. Retrieved from http://publications.gc.ca/pub?id=9.577220&sl=0

Nikl, L., Wernick, B., Van Geest, J., Hughes, C., & McMahen, K. (2016). *Mount Polley Mine embankment breach: overview of aquatic impacts and rehabilitation*. Proceedings Tailings and Mine Waste. Oct 2-5, 2015. pp. 845-856. Keystone, Colorado, USA.

Owen, J. R., Kemp, D., Lèbre, É., Svobodova, K., & Pérez Murillo, G. (2020). Catastrophic tailings dam failures and disaster risk disclosure. *International Journal of Disaster Risk Reduction*, *42*, 101361. https://doi.org/10.1016/j.ijdrr.2019.101361

Pawlowicz, R. (2008). Calculating the conductivity of natural waters. *Limnology and Oceanography: Methods*, *6*, 489-501. https://doi.org/10.4319/lom.2008.6.489

Petticrew, E. L., Albers, S. J, Baldwin, S., Carmack, E. C., Déry, S. J., Gantner, N., Graves, K., Laval, B., Morrison, J., Owens, P. N., Selbie, D., & Vagle, S. (2015). The impact of a catastrophic mine tailings spill into one of North America's largest fjord lakes: Quesnel Lake, British Columbia. *Geophysical Research Letters*, *42*, 3347-3355. https://doi.org/10.1002/2015GL063345

Potts, D., Rogers, J., Matthieu, J., & Stronach, J. (2015). *Bathymetry analysis and volume balance*. Prepared for Mount Polley Mining Corporation by Tetra Tech EBA. Report No 704-V13203212.

Pullum, L., Boger, D. V., & Sofra, F. (2018). Hydraulic mineral waste transport and storage. *Annual Review* of *Fluid Mechanics*, *58*, 157-185. https://doi.org/10.1146/annurev-fluid-122316-045027

Robertson, P. K., de Melo, L., Williams, D. J., & Wilson, G.W. (2019). *Report of the expert panel on the technical causes of the failure of the Feijao Dam* I. 12 December 2019. 81pp. Retrieved from https://bdrb1investigationstacc.z15.web.core.windows.net/assets/Feijao-Dam-I-Expert-Panel-Report-ENG.pdf (Accessed 5 April 2020)

Rotta, L. H. S., Alcântara, E., Park, E., Negri, R. G., Lin, Y. N., Bernardo, N., Mendes, T. S. G., & Filho. C.R.S. (2020). The 2019 Brumadinho tailings dam collapse: possible cause and impacts of the worst human and environmental disaster in Brazil. *International Journal of Applied Earth Observation and Geoinformation*, *90*, 102119, https://doi.org/10.1016/j.jag.2020.102119

Ruyters, S., Mertens, J., Vassilieva, E., Dehandschutter, B., Poffijn, A., & Smolders, E. (2011). The red mud accident in Ajka (Hungary): plant toxicity and trace metal bioavailability in red mud contaminated soil. *Environmental Science and Technology*, *45*, 1616-1622. https://doi.org/10.1021/es104000m

Sammarco, O. (2004). A tragic disaster caused by the failure of tailings dams leads to the formation of the Stava 1985 Foundation. *Mine Water and the Environment*, *23*, 91. https://doi.org/10.1007/s10230-004-0045-z

Santamarina, J. C., Torres-Cruz, L. A., & Bachus, R. C. (2019). Why coal ash and tailings dam disasters occur. *Science*, *364*, 526-528. https://doi.org/10.1126/science.aax1927

Saylor, J. H., & Miller, G. S. (1988). Observation of Ekman veering at the bottom of Lake Michigan. *Journal of Great Lakes Research*, *14*(1), 94-100. https://doi.org/10.1016/S0380-1330(88)71536-1

Schneider, A. R., Eadie, B. J., & Baker, J. E. (2002). Episodic particle transport events controlling PAH and PCB cycling in Grand Traverse Bay, Lake Michigan. *Environmental Science and Technology*, *36*, 1181-1190. https://doi.org/10.1021/es011262j

Segura, F. R., Nunes, E. A., Paniz, F. P., Paulelli, A. C. C., Rodrigues, G. B., Braga, G. Ú. L., dos Reis Pedreira Filho, W., Barbosa, F., Cerchiaro, G., Silva, F. F., & Batista, B. L. (2016). Potential risks of the residue from Samarco's mine dam burst (Bento Rodrigues, Brazil). *Environmental Pollution*, *218*, 813-825, https://doi.org/10.1016/j.envpol.2016.08.005.

Shandro, J., Jokinen, L., Stockwell, A., Mazzei, F., & Winkler, M. S. (2017). Risks and impacts to First Nation health and the Mount Polley mine tailings dam failure. *International Journal of Indigenous Health*, *12*(2), 84-102. https://doi.org/10.18357/ijih122201717786

Shteinman, B., Eckert, W., Kaganowsky, S., & Zohary, T. (1997). *Seiche-induced resuspension in Lake Kinneret: a fluorescent tracer experiment*. In Evans R., D., Wisniewski, J., & Wisniewski, J. R. (Eds.). (1997). *The interaction between sediments and water*. Spring, Dordrecht https://doi.org/10.1007/978-94-011-5552-6_13

SNC-Lavalin Inc. (2014*). Lower Hazeltine Creek erosion and sediment control plan*. Prepared for Mount Polley Mining Corporation, 71 pp.

Soldán, P., Pavonič, M., Bouček, J., & Kokeš, J. (2001). Baia Mare accident—brief ecotoxicological report of Czech experts. *Ecotoxicology and Environmental Safety*, *49*(3), 255-261. https://doi.org/10.1006/eesa.2001.2070

Spigel, R. H., & Imberger, J. (1980). The classification of mixed-layer dynamics in lakes of small to medium size. *Journal of Physical Oceanography*, *10*, 1104-1121. https://doi.org/10.1175/1520-0485(1980)010<1104:TCOMLD>2.0.CO;2

Stevens, C., & Imberger, J. (1996). The initial response of a stratified lake to a surface shear stress. *Journal of Fluid Mechanics*, *312*, 39-66. https://doi.org/10.1017/S0022112096001917

Stockner, J. G., & Shortreed, K. S. (1983). A comparative limnological survey of 19 sockeye salmon (*Oncorhynchus nerka*) nursery lakes in the Fraser River system, British Columbia. *Canadian Technical Reports of Fisheries and Aquatic Sciences, 1190*, 63 pp.

ten Hulscher, T. E. M., Mol, G .A. J., & Lüers, F. (1992). Release of metals from polluted sediments in a shallow lake: quantifying resuspension. *Hydrobiologia*, *235*, 97-105. https://doi.org/10.1007/BF00026203

Teodoru, C., & Wehrli, B. (2005). Retention of sediments and nutrients in the Iron Gate I Reservoir on the Danube River. *Biogeochemistry, 76*, 539-565. https://doi.org/10.1007/s10533-005-0230-6

Thompson H. D., Déry, S. J, Jackson, P. L., & Laval B. E. (2020). A synoptic climatology of potential seiche-inducing winds in a large intermontane lake: Quesnel Lake, British Columbia, Canada. *International Journal of Climatology*, 1-14. https://doi.org/10.1002/joc.6560

Valipour, R., Boegman, L., Bouffard, D., & Rao, Y. R. (2017). Sediment resuspension mechanisms and their contributions to high-turbidity events in a large lake. *Limnology and Oceanography*, *62*(3), 1045-1065. https://doi.org/10.1002/lno.10485

Van Niekerk, H. J., & Viljoen, M. J. (2005). Causes and consequences of the Merriespruit and other tailings-dam failures. *Land Degradation and Development*, *16*, 201-212. https://doi.org/10.1002/ldr.681

Veinott, G., Sylvester, P., Hamoutene, D., Anderson, M. R., Meade, J., & Payne, J. (2015). State of the marine environment at Little Bay Arm, Newfoundland and Labrador, Canada, 10 years after a "do nothing" response to a mine tailings spill. *Journal of Environmental Monitoring*, *5*, 626-634.

Vogel, A. (2013). Failures of dams –challenges to the present and the future. IABSE Symposium Report. 100. https://doi.org/10.2749/222137813807018908

Vukovic, D., Vukovic, C., & Stankovic, S. (2014). The impact of the Danube Iron Gate Dam on heavy metal storage and sediment flux within the reservoir. *Catena*, *113*, 18-23. https://doi.org/10.1016/j.catena.2013.07.012

Wang, H., Zhao, Y., Wang, X., & Liang, D. (2017). Fluctuations in Cd release from surface-deposited sediment in a river-connected lake following dredging. *Journal of Geochemical Exploration*, *172*, 184-194.

Wetzel, R. W. (2001). *Limnology* (3rd Ed.). Academic Press. London, United Kingdom. 1006 p. https://doi.org/10.1016/B978-0-08-057439-4.50009-5.

WISE (World Information Service on Energy). (2020). *Chronology of major tailings dam failures*. Retrieved from http://www.wise-uranium.org/mdaf.html (Accessed 7 April 2020)

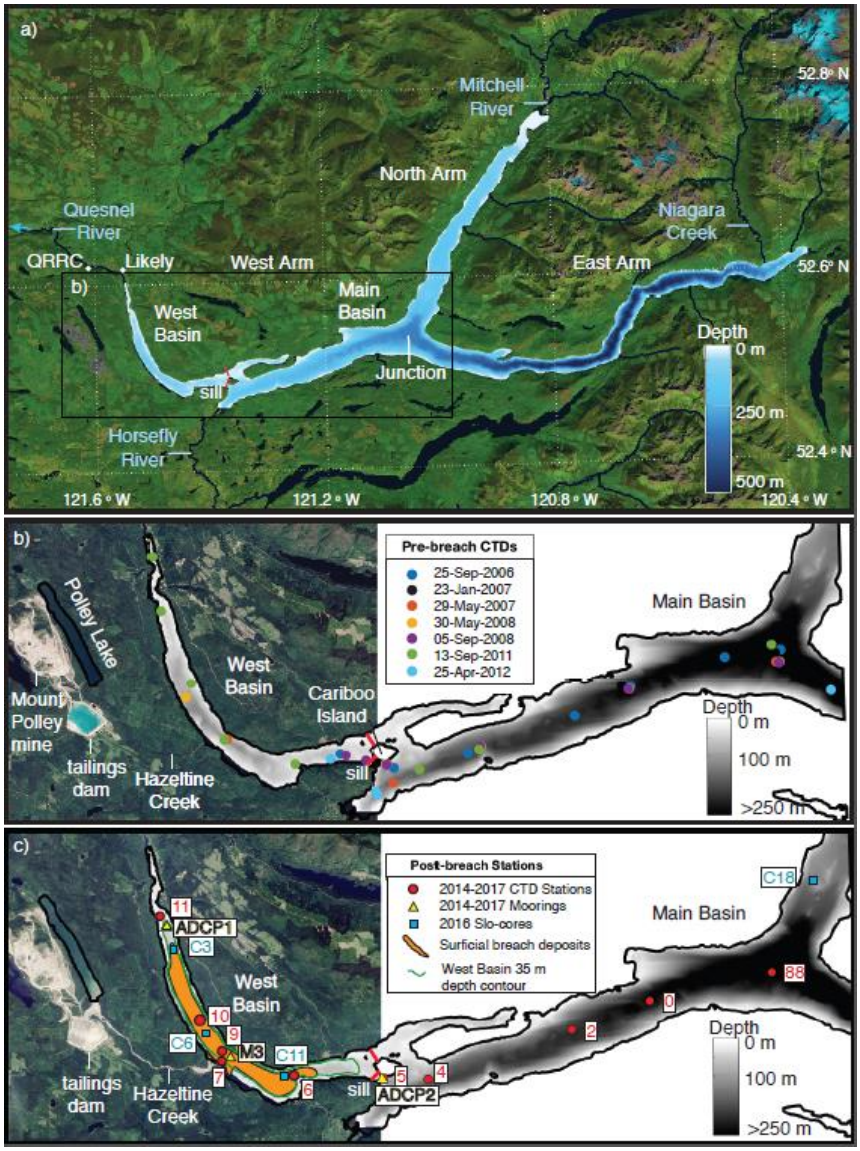

Figure 1. Map of study area. a) Shaded bathymetry of Quesnel Lake, BC, with major rivers, overlain on a LandSat image. b) Locations of West Arm pre-breach conductivity-temperature-depth (CTD) profiles overlain on 29 July 2014 LandSat image. c) Locations of West Arm post-breach repeat profile stations, moorings, slo-corer sites, and the approximate extent of the surficial breach deposit (adapted from Golder Associates, 2019), overlain on 5 August 2014 LandSat image. (Satellite images courtesy of NASA). QRRC – Quesnel River Research Station.

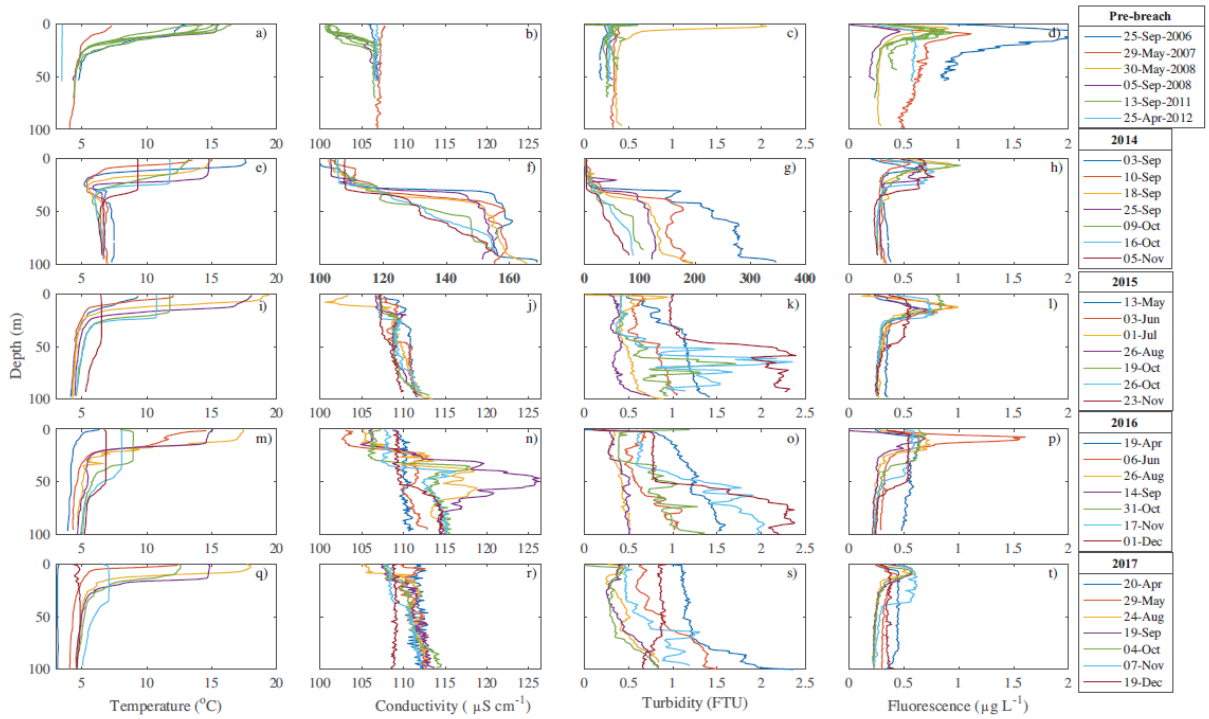

Figure 2. Water column profiles collected in the West Basin of Quesnel Lake between 2006 and 2017. Pre-spill profiles (a-d) are from any location west of the Cariboo Island sill. Post-spill profiles (e-t) were collected at Station 9 in the center of the West Basin. Note the difference in the conductivity (referenced to 25 ºC) and turbidity x-axis scales for the 2014 profiles (bold). See Figure 1 for profile locations. Only select post-spill profiles are shown to capture the range of variability but minimize clutter. Temperature and conductivity data were not available from May 2008.

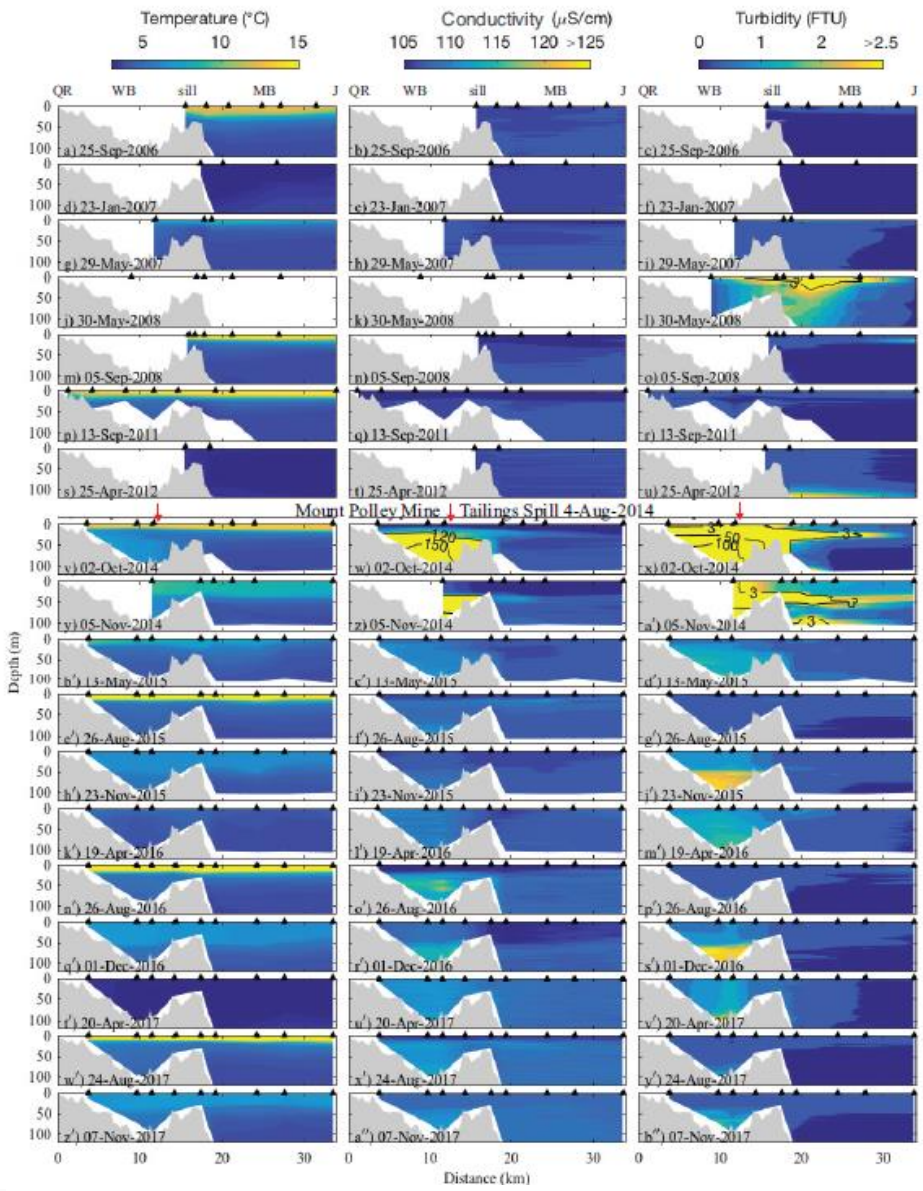

Figure 3. Timeseries of water column profile transects along the West Arm of Quesnel Lake from 2006 to 2017. The transects extend from Quesnel River (QR) to the Junction (J). WB – West Basin, MB – Main Basin. Locations of profiles are indicated (black triangles). Only select post-spill transects are shown to illustrate seasonal variation in the WB. Temperature and conductivity (referenced to 25 ºC) data were not available from May 2008.

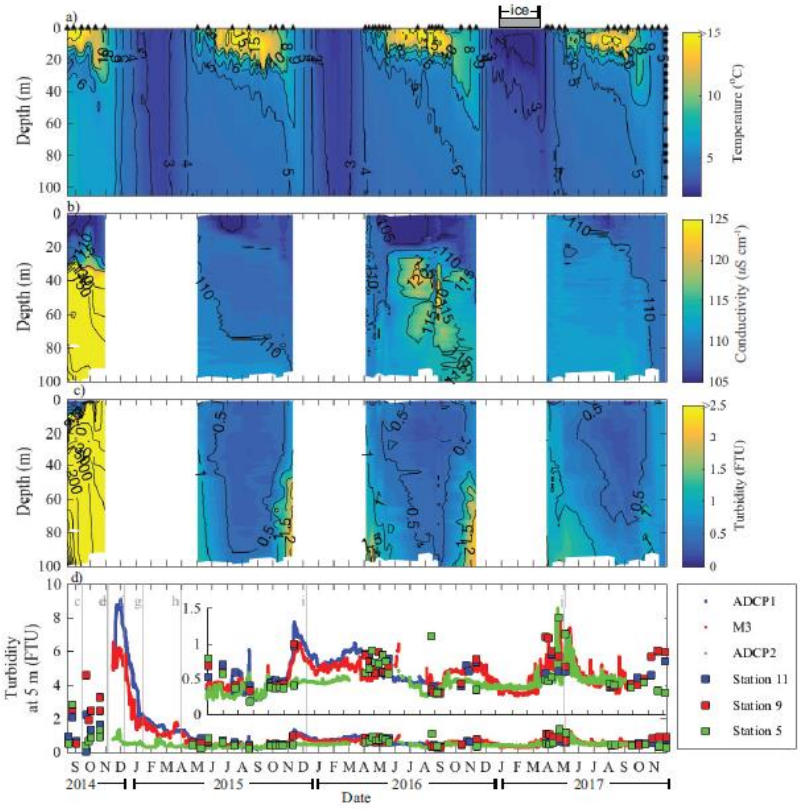

Figure 4. Timeseries of post-spill water property variation in the West Basin from 2014 to 2017. In a) temperature contours are generated from gridded water column profiles collected at Station 9 (profiling dates are indicated by black triangles) and M3 moored thermistor data (depths of thermistors are indicated by black circles). A period of ice-covered in Jan-Mar 2017 is marked. Contours of b) conductivity and c) turbidity were generated from profiles only. d) Timeseries of near-surface (5 m) turbidity in the West Basin from moorings ADCP1 (blue), M3 (red), and ADCP2 (green). Turbidity measured by profiles collected near these locations is also shown (colored squares). Inset shows small turbidity variation from June 2015 to December 2017. Vertical gray lines indicate the timing of the MODIS satellite images shown in Figure 6.

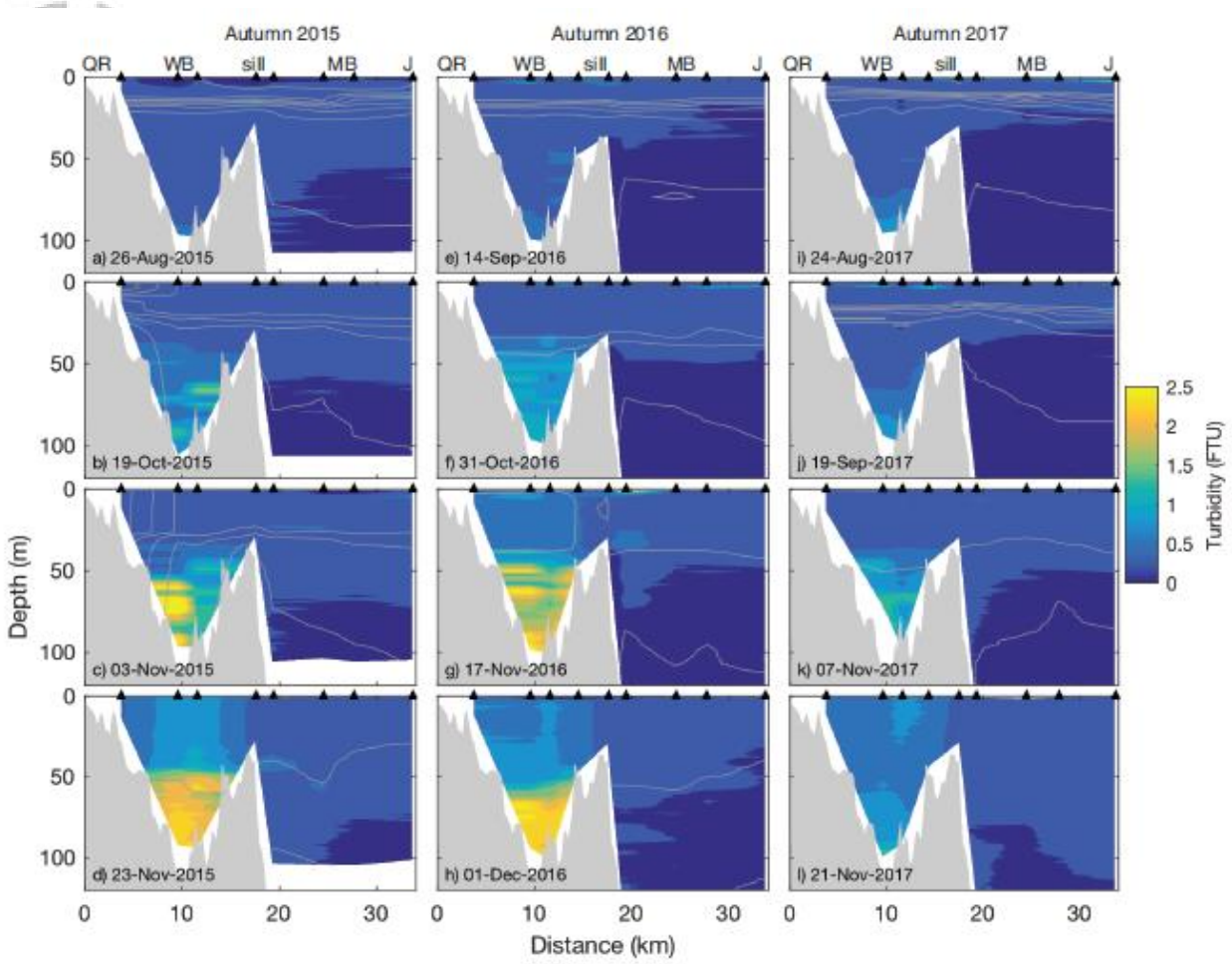

Figure 5. West Arm transects showing the seasonal turbidity increase in the hypolimnion of the West Basin during autumn 2015 (a-d), 2016 (e-h), and 2017 (i-l). Isotherms every 2°C are overlain. Note that the West Basin did not become completely isothermal to the bottom until after the final transect in 2015 and 2016. QR – Quesnel River, WB – West Basin, MB – Main Basin, J – Junction.

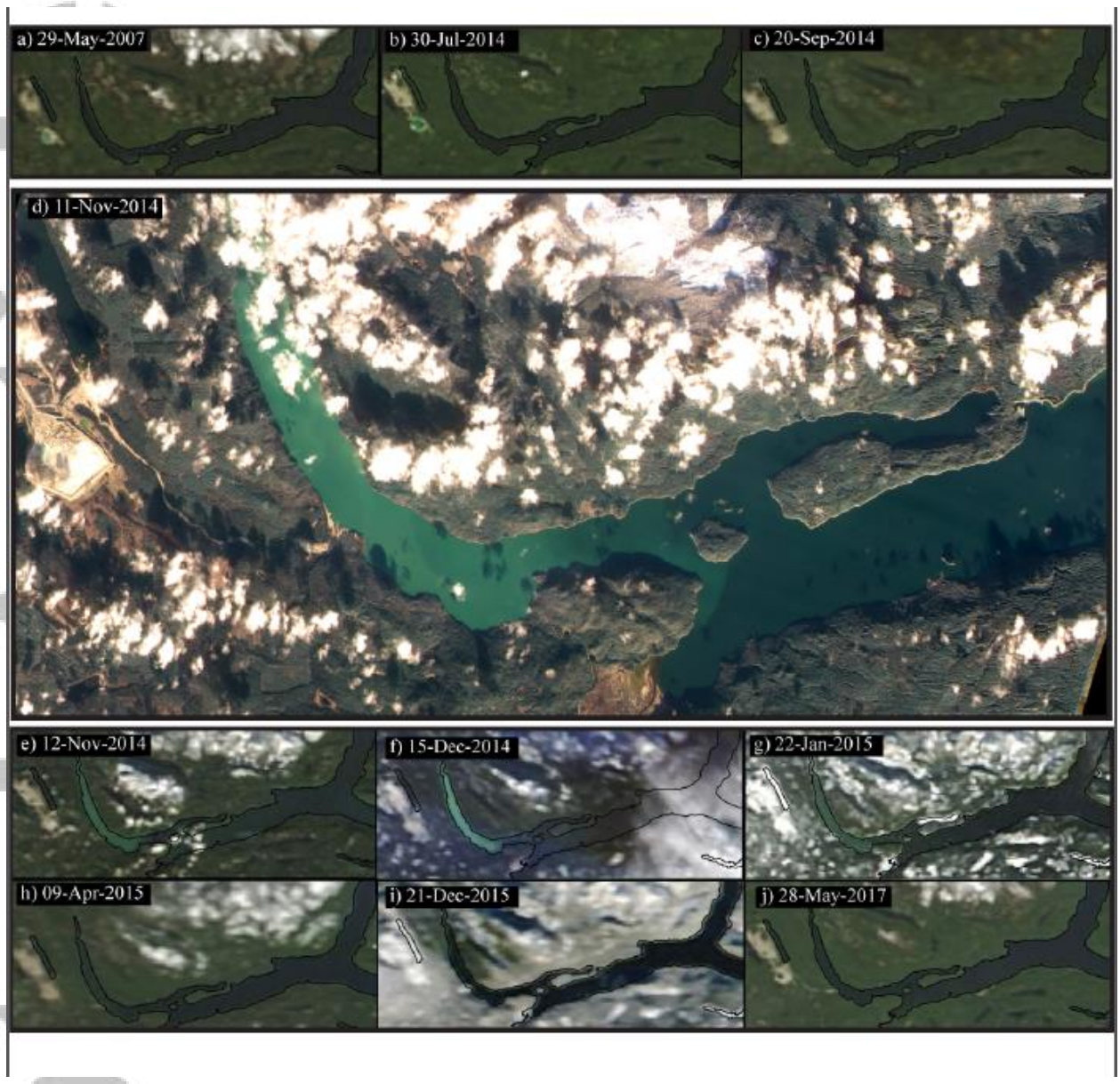

Figure 6. Timeseries of visible corrected reflectance satellite images of Quesnel Lake showing the distinct change of water color of the West Basin during autumn turnover 2014. Low (250 m) resolution Terra/Aqua MODIS imagery was obtained from NASA Worldview [https://worldview.earthdata.nasa.gov/]. The high (2 m) resolution FormoSat2 image in (d) was obtained from Apollo Mapping [https://apollomapping.com/].

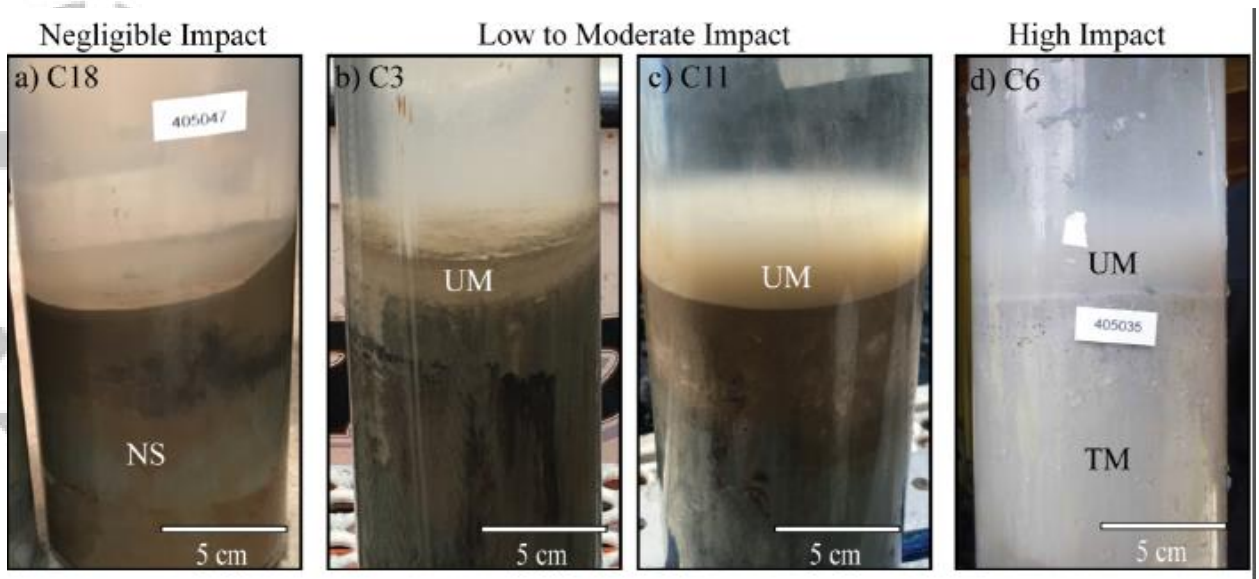

Figure 7. Images of slo-corer bottom samples collected in Quesnel Lake between 11-18 July 2016. A clear sediment–water interface is visible in core C18 (a) collected in the North Arm far away from the MPMC tailings dam breach impact site, while the WB cores (b-d) show an unconsolidated layer overlying natural sediment (cores C3 & C11) and tailings material (core C6). Cores are categorized by relative impact of breach event-related tailings deposition at each site (coring locations are shown in Fig. 1c). NS – natural sediment; UM – unconsolidated material; TM – tailings material.

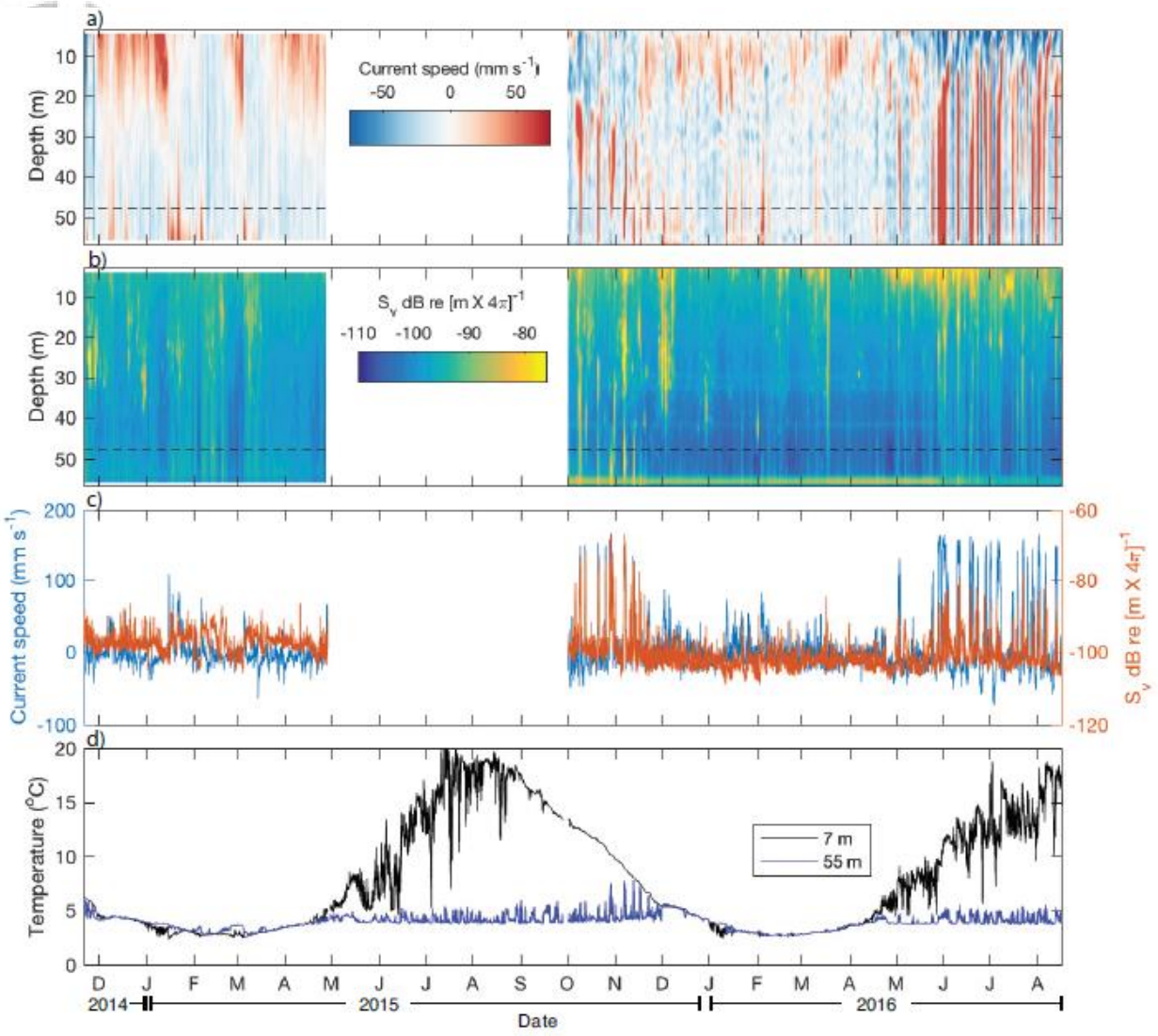

Figure 8. ADCP2 timeseries of a) current speed over the sill (positive out of the West Basin), b) backscatter intensity, c) speed and backscatter at 48 m depth bin, and d) water temperatures at 7 and 55 m depth from November 2014 to August 2016.

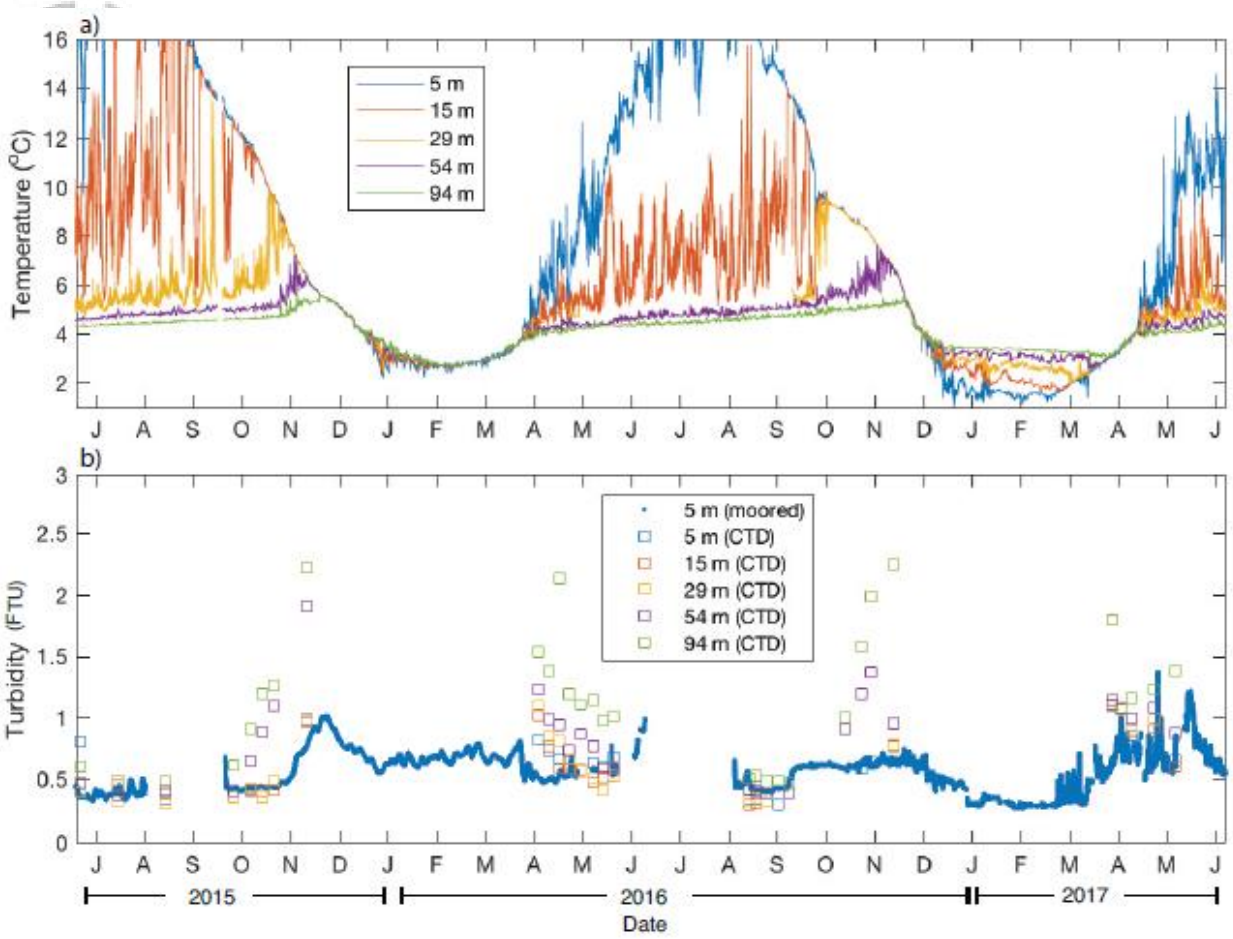

Figure 9. Timeseries of a) temperature at mooring M3 and b) turbidity at mooring M3 (dots) and conductivity-temperature-depth (CTD) Station 9 (squares) in the West Basin from June 2015 to June 2017.